NAVAL POSTGRADUATE SCHOOL

MONTEREY, CALIFORNIA

THESIS

THE NORTH ATLANTIC OSCILLATION INFLUENCE ON THE WAVE REGIME IN PORTUGAL: AN EXTREME WAVE EVENT ANALYSIS

by

Alvaro A. M. SEMEDO

March 2005

Co-Advisors: Wendell A. Nuss
Thomas H. C. Herbers

Approved for public release; distribution unlimited

THIS PAGE INTENTIONALLY LEFT BLANK

REPORT DOCUMENTATION PAGE			Form Approved OMB No. 0704-0188

1. AGENCY USE ONLY *(Leave blank)*	2. REPORT DATE	3. REPORT TYPE AND DATES COVERED
	March 2005	Master's Thesis

4. TITLE AND SUBTITLE: The North Atlantic Oscillation Influence on the Wave regime in Portugal: An extreme Wave Event Analysis	5. FUNDING NUMBERS
6. AUTHOR(S) Alvaro A. M. Semedo	
7. PERFORMING ORGANIZATION NAME(S) AND ADDRESS(ES) Naval Postgraduate School Monterey, CA 93943-5000	8. PERFORMING ORGANIZATION REPORT NUMBER
9. SPONSORING /MONITORING AGENCY NAME(S) AND ADDRESS(ES) N/A	10. SPONSORING/MONITORING AGENCY REPORT NUMBER

11. SUPPLEMENTARY NOTES The views expressed in this thesis are those of the author and do not reflect the official policy or position of the Department of Defense or the U.S. Government.

12a. DISTRIBUTION / AVAILABILITY STATEMENT	12b. DISTRIBUTION CODE
Approved for public release; distribution unlimited	

13. ABSTRACT (maximum 200 words)

Waves in the North Atlantic are strongly seasonal, and peak in the winter season. The west coast of Portugal is exposed to winter swell, generated by wind associated with North Atlantic extratropical cyclones. The track of these storms, generated near the North America east coast, is strongly influenced by the North Atlantic Oscillation (NAO). When the NAO is in its positive phase they normally track northeast and reach Western Europe well north of the Iberian Peninsula, in the British Islands or Scandinavia. However, in the negative NAO situation, the track of the storms is more zonal and south than usual, due to a weakened NAO. The characteristics of wave regime in Portugal are shown to be strongly related to the NAO phase and corresponding storm tracking. Positive NAO storms, tracking northeast towards the north of Europe, drive longer period swell from the northwest, whereas negative NAO storms have associated shorter period swell arriving to Portugal from a more westerly direction. The relation between the NAO phase and the storm tracks and the characteristics of the wave regime is investigated with ten year observations from four directional waverider coastal buoys, located off the coast of Portugal.

14. SUBJECT TERMS	15. NUMBER OF PAGES
North Atlantic Oscillation, NAO, Fetch, Waves, Portugal, Storm Tracking, Hindcast, WAVEWATCH III	106
	16. PRICE CODE

17. SECURITY CLASSIFICATION OF REPORT	18. SECURITY CLASSIFICATION OF THIS PAGE	19. SECURITY CLASSIFICATION OF ABSTRACT	20. LIMITATION OF ABSTRACT
Unclassified	Unclassified	Unclassified	UL

NSN 7540-01-280-5500 Standard Form 298 (Rev. 2-89)
Prescribed by ANSI Std. 239-18

THIS PAGE INTENTIONALLY LEFT BLANK

Approved for public release; distribution unlimited

THE NORTH ATLANTIC OSCILLATION INFLUENCE ON THE WAVE REGIME IN PORTUGAL: AN EXTREME WAVE EVENT ANALYSIS

Alvaro A. M. Semedo
Lieutenant Commander, Portuguese Navy
B.S., Portuguese Naval Academy, 1990

Submitted in partial fulfillment of the
requirements for the degree of

MASTER OF SCIENCE IN METEOROLOGY
and
MASTERS OF SCIENCE IN PHYSICAL OCEANOGRAPHY

from the

NAVAL POSTGRADUATE SCHOOL
March 2005

Author: Alvaro A. M. Semedo

Approved by: Wendell A. Nuss
Co-Advisor

Thomas H. C. Herbers
Co-Advisor

Philip A. Durkee
Chairman, Department of Meteorology

Mary L. Batteen
Chairman, Department of Oceanography

THIS PAGE INTENTIONALLY LEFT BLANK

ABSTRACT

Waves in the North Atlantic are strongly seasonal, and peak in the winter season. The west coast of Portugal is exposed to winter swell, generated by wind associated with North Atlantic extratropical cyclones. The track of these storms, generated near the North America east coast, is strongly influenced by the North Atlantic Oscillation (NAO). When the NAO is in its positive phase they normally track northeast and reach Western Europe well north of the Iberian Peninsula, in the British Islands or Scandinavia. However, in the negative NAO situation, the track of the storms is more zonal and south than usual, due to a weakened NAO. The characteristics of wave regime in Portugal are shown to be strongly related to the NAO phase and corresponding storm tracking. Positive NAO storms, tracking northeast towards the north of Europe, drive longer period swell from the northwest, whereas negative NAO storms have associated shorter period swell arriving to Portugal from a more westerly direction. The relation between the NAO phase and the storm tracks and the characteristics of the wave regime is investigated with ten year observations from four directional waverider coastal buoys, located off the coast of Portugal.

THIS PAGE INTENTIONALLY LEFT BLANK

TABLE OF CONTENTS

THIS PAGE INTENTIONALLY LEFT BLANK

LIST OF FIGURES

LIST OF TABLES

THIS PAGE INTENTIONALLY LEFT BLANK

ACKNOWLEDGMENTS

Data for this study was collected mainly off the coast of Portugal. I respectfully thank the Oceanography Department of the Portuguese Navy's *Instituto Hidrografico* for supplying me with all the data used in this thesis, and for assisting me throughout my work. In particular, I would like to thank Commander Carlos Ventura Soares and Mrs Mariana Costa for their support.

I sincerely thank my advisors, Professors Wendell Nuss and Thomas Herbers, for their expert guidance, and for enabling me to fly in pursuit of my goals. Their advice, enthusiasm and support were invaluable. I especially want to thank them for allowing me to present my work at the annual meeting of the American Meteorological Society. I'm also very grateful to Dr. Joao Teixeira (of the Naval Research Laboratory) for his advice and support, and to LCDR Juan Conforto, for helping me with the buoy data from Spain, but most of all for their friendship. My deepest thanks go, as well, to Mr Paul Wittmann for his ongoing assistance in setting up and running the WAVEWATCH III model for the hindcast experiments reported here. Also, I give my heartfelt thanks to Mr Paul Jessen, who assisted me enormously with MATLAB programming, and also helped to preserve my sanity on many occasions.

I want to express my undying gratitude, especially, to my beautiful wife, whom I love more than anything in the world, for her support and everlasting encouragement, and for seeing me as being something more than I'll ever be. Her willingness to follow me from one side of the world to

the other — from Stockholm to Monterey, en route to Lisbon, where we will be happier than ever – allowed us to enjoy a lifetime adventure that we will remember forever. I also want to thank my American friends, Matt Moore, Justin Reeves, Tom Moneymaker and Sim James for making me feel at home, for their dry sense of humor, and for our unforgettable coffee breaks. May we meet again in the future.

I. INTRODUCTION

A. THE NORTH ATLANTIC OSCILLATION

The west coasts mid-latitude continental land masses tend to have a rougher wave climate than do land masses on the east coasts. At these latitudes, the mean prevailing surface wind is from the west (called “westerlies”), and, therefore, the west coasts experience long fetches and hence higher wave regimes. The North Atlantic Ocean basin is no exception to this rule. The west coast of Europe experiences the longest and highest waves in the Atlantic Ocean mainly during the winter months (Young, 1999). The relatively narrow configuration of the Atlantic restricts the propagation of swells from the south into the Northern Hemisphere, in contrast to the wide Pacific Ocean basin. Hence the North Atlantic extratropical cyclonic storms are the main driving force behind the winter wave regime on the west coast of Europe.

Waves in the North Atlantic are strongly seasonal, peaking in the winter months. Significant wave height in the northeastern part of the Atlantic also exhibit exceptionally high interannual variability in the winter, with the monthly average varying considerably from one year to the next by up to a factor of two (Wolf, 2002). These wave height anomalies are to a large extent associated with the North Atlantic Oscillation (NAO) and its impact on the cyclogenetic processes and storm tracking over the North Atlantic Ocean (Wolf, 2002). The NAO is regarded as the primary teleconnection over the North Atlantic (Rogers, 1997) and is linked to observed climatological and

oceanographic variability over Eastern North America, the North Atlantic and the Eurasian continent (van Loon and Rogers, 1978). In simple terms, the NAO corresponds to a large scale meridional oscillation of atmospheric mass between the Icelandic Low and the subtropical Azores High, being a measure of the strength of the North Atlantic Westerlies (Hurrel, 1995). Trigo *et al.* (2002) notes that Walker (1923) was probably the first to notice a simultaneous tendency between the strengthening of the Icelandic low pressure system and the Azores subtropical high, which he named North Atlantic Oscillation, or NAO.

The strength of the NAO is described by an index. A positive NAO index will show a stronger than usual sub-tropical high pressure center near the Azores, and a deeper than normal Icelandic low. This increase in the pressure difference will result in more and stronger winter storms crossing the North Atlantic. It will also exhibit a pronounced north–eastward orientation of storm tracks, parallel to the North American East coast (Lao, 1988; Rogers, 1997), with a cyclone maximum just south of the climatological Icelandic Low (Serreze *et al.*, 1997). The consequences are milder and wetter maritime winters in Iceland, Scandinavia, and parts of Northern Europe, and colder and dryer winters in Southern Europe, from the Iberian Peninsula throughout the Mediterranean Sea basin (Ulbrich *et al.*, 1999). In addition stronger westerlies across the North Atlantic can be observed.

On the other hand, a negative NAO index mode is characterized by a weak Icelandic low and a weak subtropical Azores High. The reduced pressure gradient in

such situations will lead to fewer and weaker storms crossing the North Atlantic on a more east-west path, approximately along 45° N latitude (Hurrel, 1995). These southern, and more zonal, storms bring higher than normal precipitation into the Iberian Peninsula and Southern Europe, as well as colder and dryer weather into the Scandinavian Peninsula and Northern Europe (Ulbrich *et al.*, 1999) (Figure 1).

Geostrophic balance implies that a high NAO index (i.e., a stronger sea level pressure [SLP] gradient between Iceland and the Azores), will intensify the surface westerlies, thus enhancing the cyclonic activity over the Atlantic (Carlton, 1988). On the other hand, a negative NAO index (i.e., a weaker SLP gradient) will result in weaker surface westerlies. In fact, during winters characterized by a relatively high NAO the surface westerlies coming into Europe can be up to 8 m/s stronger than those observed during lower NAO winters (Rogers, 1997).

Over the last 150 years the NAO index time series show a broadly consistent picture of long-term behavior. Since 1970, especially in the last 25 years, the NAO index has shown a trend of unusually large positive values, (see the dashed green line in Figure 2). This increase not only has direct consequences for the average wave height, but has also been linked to global warming (Grevemeyer *et al.*, 2000). However, some authors find it premature to jump to such conclusions. Nevertheless, over the last 30 years, wave measurements across the North Atlantic show an increase of 0.6 meters in the average significant wave height (Wolf, 2002).

The role of the ocean, especially the sea surface temperature (SST), in regulating the NAO has been the subject of several studies (e.g., Canyan, 1992, and Kushnir, 1999). However, there is little agreement over what that role is, therefore, it still remains controversial. Nevertheless, it is widely recognized that the NAO has an important forcing role in the North Atlantic Ocean. In his historic study of air-sea interaction over the North Atlantic, Bjerkens (1964) examined the relationship between anomalies in the North Atlantic SLP and SST, suggesting that the interannual SST anomalies are locally driven by changes in the heat flux from the atmosphere. On the decadal timescale, however, changes in the ocean circulation, and hence ocean heat transport, may also play an important role in regulating the NAO. Some authors also suggested that there is link between the NAO index and the frequency and duration of atmospheric blocking events over the North Atlantic (Shutts, 1986; Hurrel, 1996, Huang *et al.*, 2000). What is less clear, however, is whether the blocking events are causing periods of low NAO index, or if they are merely symptoms of the weakened polar vortex associated with a low NAO index. Nevertheless, the blocking is likely important in the synoptic and sub-synoptic activity over the Atlantic in affecting storm tracks.

The upper air has a strong influence in steering surface features. Since the subtropical jet tends to coincide with the pathway of the storm on the surface, the NAO phase affects both the intensity and location of the sub-tropical jet, as well as the storm tracks across the North Atlantic basin. Years having a positive NAO phase

tend to have stronger storms, penetrating further to the North, and with a stronger and more poleward path of the subtropical jet. Conversely, years in which the atmosphere is in a negative NAO phase have weaker and more zonal storms and subtropical jet.

The influence of the NAO in the strength and track of the storms leads to the suggestion that there may be a robust relationship between wave height anomalies and the NAO index. In a high positive NAO, one can think of a large sea accumulating and propagating into the eastern edge of the North Atlantic basin, as it is driven into the west coasts of Ireland and Scotland, or into the North Sea, by strong and persistent westerlies. During negative NAO events, on the other hand, the winds will be weaker, and as a consequence, the less developed sea will be driven primarily into the Iberian Peninsula or the Biscay Gulf.

Wolf (2002) showed that massive fluctuations in the wave climate over the North Atlantic (particularly in the northeastern sector) are related to the behavior of the NAO, defining it as the greatest single source of interannual variability. In certain situations either unusually large waves in the North East Atlantic or unusually small waves south of the Azores or in the Labrador Sea are associated with a positive phase of the NAO). For example, after several rough winters in the first half of the 1990s, a drop of approximately two meters in the North Atlantic winter’s significant wave height in the 1995/1996, was correlated with a sudden switch to a negative state of the NAO. In fact, the difficulty in

defining a secular trend in the wave heights in the 1990s was due primarily to the erratic behavior of the NAO in that decade (Figure 2).

Most modern NAO indices are derived either from 1) the difference of SLP between two stations close to the centers of the Icelandic Low and the Azores subtropical High, or 2) the application of principal component (PC) analysis to the time series of the leading empirical orthogonal functions (EOF) of the SLP. In Iceland, either *Stykkisholmur* or *Akureyri*, in Iceland (locations separated by ~50 km), are used as the northern station, whereas for the southern stations *Ponta Delgada* (Azores, Portugal), Lisbon (Portugal), *Cadiz* (Spain) and Gibraltar have all been used for the southern stations at various times. Jones *et al.* (2003) compared various station-based indices and noted that the major advantage of these indices is that they extend back to the mid-19th century. On the other hand, one disadvantage, as noted by Hurrel *et al.*(2003), is that they are fixed in space, i.e., when considering the fact that the NAO centers of action move through the annual cycle, these indices can only capture the NAO variability for parts of the year (mostly during the winter time). Additionally, individual stations may be affected by small-scale meteorological phenomena that are not directly related to the NAO, thus giving false readings (Hurrel and van Loon, 1997). An advantage of the PC analysis is that such indices are more optimal representations of the full NAO spatial pattern. Nevertheless, depending on the data source, since they are based on gridded SLP data, they can only be computed for parts of the 20th century.

B. WIND-WAVE PREDICTION

Although considerable empirical knowledge on the generation and decay of ocean waves has been accumulated during the last century, the dynamic processes were poorly understood until two independent, but complementary, theories were developed by Phillips (1957) and Miles (1957). Phillips' theory of wind-wave generation is based on the assumption that turbulent pressure fluctuations in the atmosphere are not affected by the waves and are advected over the water surface with the wind speed U. Phillips showed that resonance between the advected pressure and waves that travel at the same speed explains the excitation and initial growth of waves on an undisturbed water surface. Nevertheless, this simple mechanism does not explain the continued growth of wind waves.

Once waves are generated on the water surface, their presence modifies the air flow. Miles (1957) analyzed this effect on the coupled air-water motion using the simplest inviscid form of the stability theory, *i.e.,* Rayleigh's equation in the air and Laplace's equation in the water, with proper matching and boundary conditions. In this model, turbulence has no explicit participation in the momentum transfer to the water surface, which happens entirely through pressure forces. The resulting wave number spectrum of the surface gravity waves grows much more rapidly than it does in the case of the Phillips resonance mechanism. Phillips' and Miles' mechanisms can be combined to describe the wave generation process from initial growth to full development. This theory, reviewed and

supplemented by many authors, remains the cornerstone of the theoretical understanding of wind-wave generation.

The first operational forecast model of ocean waves dates back to World War II, when Sverdrup and Munk, for the invasion of Normandy in 1945, attempted to predict waves in the English Channel. Their study later declassified and published (Sverdrup & Munk, 1947), was based on a semi-empirical wave forecasting relationship that made extended use of graphic solutions. Subsequently, Gelci *et al.* (1957) developed the first modern wave prediction model that made use of the transport equation or energy balance equation:

$$\frac{\partial F}{\partial t} + \vec{v}.\nabla F = S \equiv S_{in} + S_{nl} + S_{ds} \qquad (1)$$

where $F(f,\theta;\vec{x},t)$ is the two dimensional wave spectrum, f is frequency, θ is the direction of propagation, $\vec{v}$ is the deep water wave group velocity and S is the net source function (S_{in} is the input by the wind, S_{nl} the nonlinear transfer and S_{ds} the dissipation).

At that time, little was known about the source function components. However, considerable progress was made soon thereafter, including the advent of the Phillips-Miles generation theory (a simple model for wave breaking that assumes a universal saturation spectrum [Phillips, 1958]), and the derivation of the nonlinear energy transfer due to resonant wave-wave interactions (Hasselmann,1962). These and other developments provided the theoretical

framework was available for the wave models that were developed in the 1960s, and further modified in the 1970s.

The first generation of wave models, developed in the 1960s and early 1970s, used an input source function of the form:

$$S_{in} = A + B \cdot F \qquad (2)$$

where A represents the Phillips external turbulent pressure forcing, and $B \cdot F$ is the linear feedback mechanism proposed by Miles (or Jeffrey [1925] early sheltering theory). The dissipation source term S_{ds} was usually treated as an on-off limiter of the growth in the wind sea region of the spectrum. This limiter was effective only when the spectrum reached a prescribed level. The nonlinear transfer S_{nl} term was incorporated using a simple parameterization scheme or entirely neglected. There were doubts that these models fully represented the physics of wave generation. In fact, for growing wind seas, the forecasting of the modeled spectrum was restricted to wave components close to the spectral peak. Today it is accepted that a universal high-frequency equilibrium spectrum does not exist.

A balance between wind input and whitecapping (dissipation) in the high frequency region of the spectrum does not exist because it is coupled via the nonlinear transfer mechanism to the low frequency region of the spectrum. Important deficiencies of these first generation

models include an overestimation of the wind input and underestimation (or neglect) of the nonlinear energy transfer (WAMDI, 1988)

In the early 1970s, several experiments, mainly the Joint North Sea Wave Project (JONSWAP) (Hasselmann *et al.*, 1973), became the basis for a second generation of wave models. The principal source of energy during the main growth phase of waves on the low-frequency forward face of the spectrum was now believed to be the nonlinear transfer, instead of the direct wind forcing. It was also discovered that the nonlinear transfer controls the shape of the spectrum, including the development and overshooting of a sharp peak that migrates toward lower frequencies. Although an improvement in forecasting capabilities was achieved, these heavily parameterized second generation models still had a simplified view of nonlinear transfer, and did not handle the transition between windsea and swell properly.

The shortcomings and pitfalls of the first and second generation wave models were thoroughly examined in the international wave-model testing and intercomparison program, known as SWAMP (1985). This study concluded that none of the existing models up to the early 1980s were applicable for all types of windfields and, most significantly, were not reliable in extreme situations. The SWAMP report proposed that the scientific community should go further and develop a third generation wave model; models in which the wave spectrum could be evaluated explicitly by integration of the basic spectral transport equation, without any prior restriction on the spectral shape. Simultaneously, improvements in the numerical

computation of the Boltzman-type integral of nonlinear transfers became available. These improvements led to the first third generation wave model WAM (WAMDI Group, 1988). The source function was still represented as a superposition of wind input, nonlinear transfer and dissipation, as in (1), however significant changes where introduced in the parameterization of the source components.

WAVEWATCH III (Tolman, 2003) is a full-spectral, state-of-the-art, third generation ocean wave model that was developed at the Marine Modeling and Analysis Branch (MMAB) of the Environmental Modeling Center (EMC) of the National Centers for the Environmental Prediction (NCEP). It has its roots in the previous WAVEWATCH I and WAVEWATCH II models, developed at Delft University of Technology in the Netherlands, and NASA Goddard Space Flight Center. This model includes numerous improvements in its structure, its governing equations, numerical methods and physical parameterizations. WAVEWATCH III version 2.22 (Tolman, 2003) was used in the hindcast experiments performed in this study.

The net source term used in WAVEWATCH III is the same as in (1), with an additional term, S_{bot}, to account for bottom friction in shallow water. The nonlinear wave-wave interactions in term S_{nl} are modeled using the discrete interaction approximation (DIA, Hasselmann *et al.*, 1985) and the Webb-Resio-Tracy method (WRT, Webb [1978], Tracy and Resio [1982] and Resio and Perrie [1991], see in Tolman [2003] for more details). The input and dissipation terms, S_{in} and S_{ds}, are treated as a collective source term, since

they are inter-connected (Tolman, 2002). The parameterization used is based on the argument that the dissipation processes for frequencies at and below the spectral peak are different from those occurring at high frequencies. For this reason, the WAVEWATCH III dissipation term contains two different components, one for each of the two different frequency regimes.

C. PURPOSE OF THE STUDY

Portugal occupies a narrow north-south strip along the Atlantic flank of the Iberian Peninsula in the southwest corner of Europe, between parallels 37° N and 42° N. The 500 kilometer long west coast of Portugal faces the North Atlantic, is exposed to winter swell generated by North Atlantic mid-latitude cyclones. Under the appropriate meteorological conditions, the significant wave height can reach values higher than 9 meters, with maximum wave heights sometimes higher than 15 meters. The observed swell arrival directions are clearly related to the track of the storms across the North Atlantic (Costa, personal communication, 2004). As mentioned above, the track of the North Atlantic storms is greatly determined by the NAO, which makes the type of swell that reaches the coast of Portugal highly dependent on the NAO phases. Positive NAO index storms tend to track more in a north-east direction, with stronger westerlies, reaching land-fall in Northern Europe and Scandinavia, far away from Portugal. On the other hand, negative NAO index storms track more south, in an east-west direction, frequently occluding over the Iberian Peninsula. However, such storms are often associated with weaker wind regimes. In these situations, the storm and the swell can be coupled, causing them to

propagate at approximately the same speed, towards the west coast of Portugal. With such a long favorable fetch and steady winds blowing in the same direction for several days, extremely high swell may be registered near the coast, often resulting in a severe impact on harbors and other coastal structures.

The recent positive NAO trend (i.e., over the last 25 years) has been linked to the increasing wave heights over the North Atlantic. Portugal's coast has not been an exception to this bias, and 25 years of wave monitoring have shown an increase in storm frequency, along with a trend of increasing wave heights (Costa, personal communication, 2004).

The purpose of this study is to investigate the relation between the NAO phase and the storm tracks and the characteristics of the wave regime off the coast of Portugal. Wave data gathered over a ten year period, by four Directional Waverider buoys off the coast of Portugal are analyzed in relation to the storm tracks and the NAO index. By making this comparison this thesis intends to aid in understanding the changes in the swell characteristics observed in response to changes in the atmospheric circulation. Additional data from a directional Seawatch buoy off the coast of *Galicia*, Spain from 1998 until the present are also used in this study. Hindcast experiments using the National Centers for Environmental Prediction and National Center for Atmospheric Research global reanalysis (henceforth designated NCEP/NCAR reanalysis) (Kalney *et al.*, 1996) winds and the WAVEWATCH III model were performed

to retrieve the characteristics of the wave field on the coast of Portugal under specific conditions.

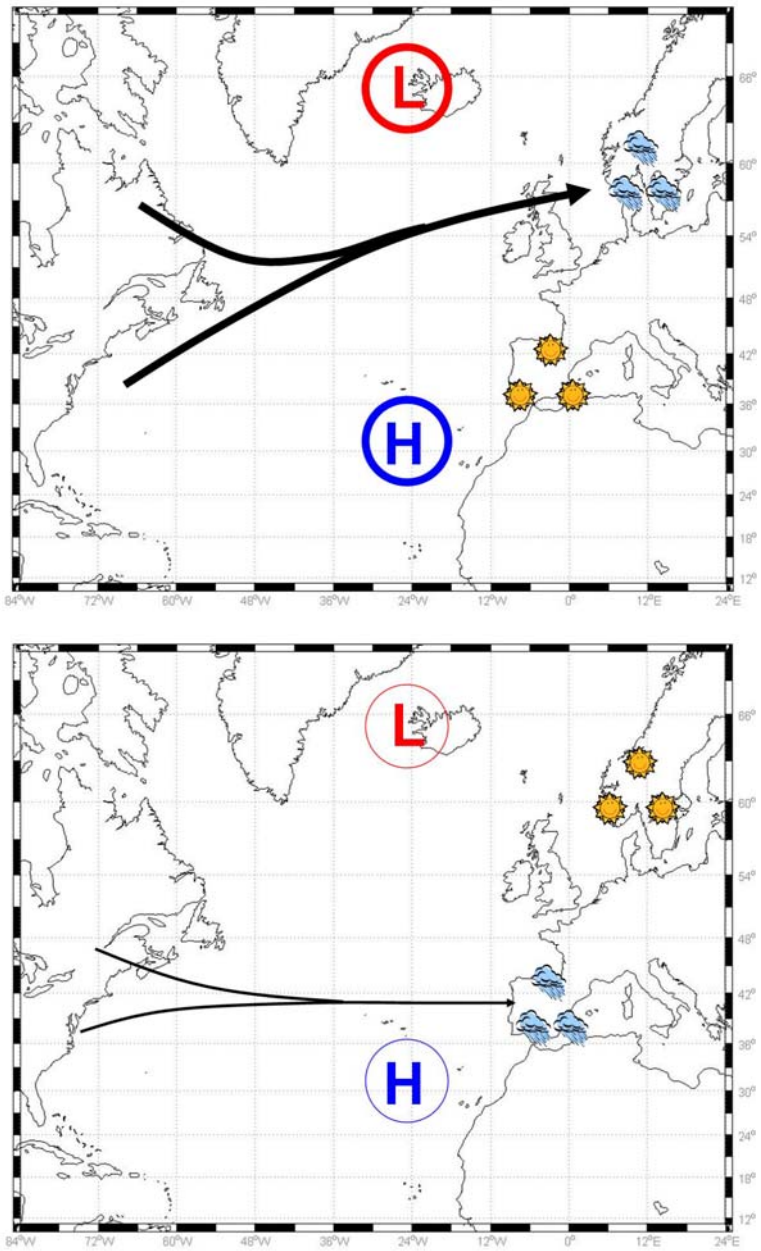

Figure 1. Storm tracks as a function of the NAO phases and rain fall regimes over North and South Europe.

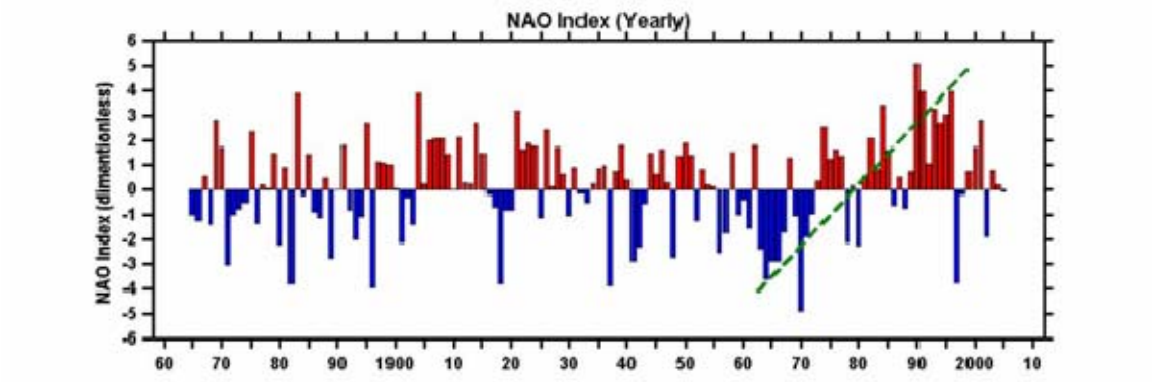

Figure 2. Normalized yearly station based NAO index (*Stykkisholmur*, Iceland and Gibraltar) from 1864 to 2004.

II. DATA SETS AND METHODOLOGY

A. BUOY DATA

1. Buoy Data – Portuguese Coast

The buoy datasets used in this study were provided by the Portuguese Navy's *Instituto Hidrográfico* (IH). The study focuses on ten years of wave data time series, from 1994 to 2003. The data were collected by four offshore Datawell Directional Waverider buoys. These buoys are permanently deployed wave-measuring instruments, owned and maintained by the IH, and are part of the Portuguese wave monitoring net. All buoys are moored in about 100 meters depth and in the vicinity of harbor entrances. The IH has been collecting wave data systematically since 1979 with the objective of studying and monitoring the wave climate off the coast of Portugal.

Three of these buoys, Leixões ("P1"), Sines ("P2"). And Faro ("P3"), are moored off Portugal's mainland coast. The fourth, Funchal ("P4", is moored south of the Madeira Island. Buoys P1 and P2 are moored on the western coast of Portugal, facing the prevailing Northwest incoming swell (Pontes *et al.*, 1997). The remaining buoys, P3 and P4, are moored on the south coast of Portugal's mainland and south of Madeira Island, respectively, and therefore are more sheltered from the Northwest swell (Figure 3).

Buoys P1, P2 and P3 are moored on sandy bottoms, gently sloping alongshore uniform bathymetry, and relatively close to the coast (Table 1). Buoy P4 is moored on a rocky bottom, with a slightly more complex bathymetry than the other three (Table 1).

Datawell Directional Waverider buoys are the world's standard for measuring wave height and direction, measuring horizontal and vertical sea surface displacements by means of a 3-component accelerometer. The accelerometer is mounted on a gravity-stabilized platform that is suspended in a fluid-filled plastic sphere located at the base of the buoy. The buoy has an onboard compass and tilt sensors, designed to give its orientation in three dimensions. The measured buoy accelerations are processed onboard and converted into displacements. The buoy's internal processor controls the timing of data recording and processes the data in near 'real time' to provide a set of standard sea-state parameters and spectra.

During normal fair-sea conditions, data were collected every three hours over a period of thirty minutes, from all four buoys. During storm conditions (i.e., when significant wave height was higher than 5 meters for buoys P1 and P2 and higher than 3 meters for buoys P3 and P4) data were collected nearly continuously, for periods of 30 minutes, with short ten minute intervals to allow for internal processing and transmission of the data to shore. The data were collected at a 1.28 Hz rate. The spectral data (energy density and directional moments) was computed for 127 frequency bands, from 0.005 Hz to 0.635 Hz, with a band width of 0.005 Hz.

2. Additional Wave Data – *Galicia* (Spain) Coast

Additional wave data from the west coast of *Galicia*, Spain, collected from an offshore directional Seawatch buoy, in the vicinity of Cape Silleiro, Rayo Silleiro

("E1"), (Figure 3), was provided by the Spanish Port Authority (*Puertos del Estado*) and the Spanish Navy Hydrographic Services.

This data was used only for comparisons with model predictions in the hindcasts, since the buoy has only been in operation since July of 1998. Buoy E1 was moored on a similar sandy gently sloping alongshore uniform bottom as buoys P1 to P3, but farther away from the coast (Table 1).

Buoy	Depth (m)	Latitude (North)	Longitude (West)
P1	83	41° 18.93'	008° 59.09'
P2	97	37° 55.36′	008° 55.80′
P3	93	36° 54.38′	007° 53.97′
P4	100	32° 37.32′	016° 56.75′
E1	323	42° 07.20	009° 24.00

Table 1. Directional buoys used in the study.

B. ATMOSPHERIC DATA

The wind data utilized to drive the wave model hindcasts was provided by the six hour, 2.5 degree, horizontal resolution NCEP/NCAR reanalysis. The basic approach of the NCEP/NCAR reanalysis is to use a frozen, state-of-the-art analysis and forecast system, and perform data assimilation using past data (reanalysis). In this way, perceived climate jumps associated with changes in the data assimilation process are eliminated. The result is a research quality dataset that is suitable for many uses, including weather and short term climate research. The NCEP/NCAR reanalysis was also used to retrieve the synoptic background behind the different storms analyzed in this study, allowing a qualitative characterization of the

weather at the surface in the North Atlantic during the different case studies.

The surface wind fields for each hindcast were generated by interpolating the wind at the lowest σ level of the data (~30 meters) from 2.5 degrees to a grid spacing that would be used in the wave model domain (0.25 degrees). Since the JONSWAP experiment (Hasselmann *et al.*, 1973) the wind at ten meters height above the sea surface, i.e., U_{10}, has been frequently used to force wave prediction models. Here, we use the NCEP/NCAR reanalysis surface winds (lowest σ level) which generally correspond to elevations of about 30 meters and thus can be considered a reasonable approximation of U_{10}.

C. NORTH ATLANTIC OSCILLATION DATA

The NAO indices used in this study (yearly, monthly and daily) were computed by the National Oceanic and Atmospheric Administration (NOAA) using the NCEP/NCAR reanalysis (2.5 degree horizontal resolution). NOAA computes and updates NAO indices daily and makes them available on-line. These indices were constructed by projecting the daily and monthly mean 500 hpa height anomalies onto the ten leading EOF modes. Both time series were normalized by the standard deviation of the monthly index.

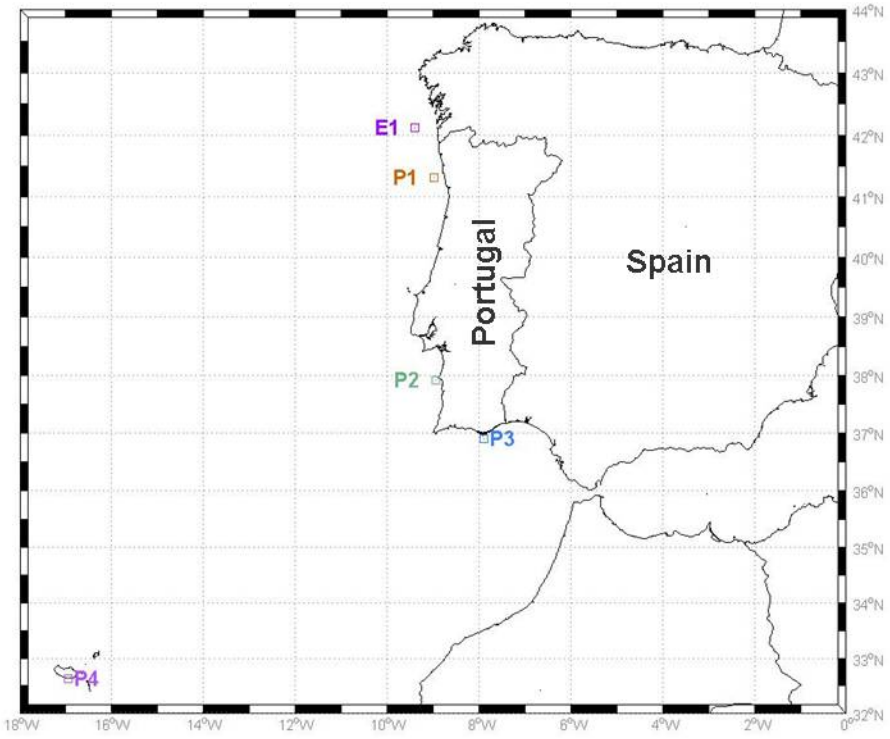

Figure 3. Buoys used in the study.

THIS PAGE INTENTIONALLY LEFT BLANK

III. CASE STUDIES

A. SELECTION AND CLASSIFICATION CRITERIA

In order to properly choose the appropriate extreme storms to be used as case studies, a selection criterion was needed. Since, to the knowledge of the author, there was no storm wave classification criterion used by the Portuguese Weather Services (*Instituto de Meteorologia*) or in the Portuguese Navy IH, a simple criterion based on the significant wave height at buoys P1 and P2 was chosen. The storms were classified as extreme if the measured significant wave height at buoys P1 or P2 was consistently higher than 7 meters. This criterion was then applied to ten years of significant wave height time series for buoys P1 and P2. These buoys were chosen to be used in the storm selection since the wave climatology off the coast of Portugal, based on more than 25 years of wave monitoring, has shown that the highest waves are consistently measured on the West coast (Costa, personal communication, 2004), rather than in the sheltered location of buoys P3 and P4 . The storms also tend to be of longer duration at these two buoys, ranging from one to several days.

The duration of the storms was defined as the longest consecutive period of significant wave height higher than 5 meters measured at either buoys P1 or P2. The peak of the storm was defined as the time at which the highest significant wave height occurred at any of the four buoys. A ten day window of time, approximately centered at the significant wave height peak of each storm, was chosen as the analysis time period for each case study. For each

storm, and for each of the four buoys, the following wave parameters were analyzed: significant wave height, peak period (1/spectral peak frequency), mean direction (at the peak frequency), directional spreading (also at the peak frequency) and estimates of the frequency-directional spectra computed using the Fast Fourier Transform (FFT) algorithm. A FFT was applied to the displacements measured by the buoys to transform the data from the temporal domain to the frequency domain, further allowing the computation of the desired wave parameters (Tucker, 2001).

B. CASES SELECTED

Based on the selection criterion, seven extreme storms were examined from October 1993 to April 2004 (Table 2).

			Significant wave height (m)	
Case	**Date**	**Duration (hours)**	**P1**	**P2**
1	Feb 1994	57:10	8.76	6.42
2	Nov 1997	53:00	6.27	7.65
3	Dec 1998 Jan 1999	38:50	8.8	7.95
4	Oct 1999	49:16	7.81	7.14
5	Jan 2002	27:35	7.72	7.54
6	Dec 2002	49:57	7.71	8.21
7	Oct Nov 2003	44:54	9.7	6.59

Table 2. Cases selected based on the storm classification criteria.

A ten day analysis time period was used as the time frame to examine the North Atlantic synoptic background for each of the case studies. The six hourly NCEP/NCAR reanalysis SLP and surface wind fields across the North

Atlantic were compiled for an extended, 14 day period (four days prior to the ten day time window) to allow for the propagation of swell generated further away from the coast of Portugal, which can take two to three days to reach the Iberian Peninsula.

For each of the seven case studies, the daily and monthly NAO indices were retrieved with the purpose of investigating the relation between the NAO, and therefore the strength of the westerlies at the surface and the storm track, and the wave field measured on the coast of Portugal. Since the ten day time period used for wave analysis was shorter than the month-long period used to determine the monthly NAO index (Figure 4), a special ten day based NAO index (henceforth designated ten day NAO index) was computed, to avoid possible biasing. This index was computed by averaging the daily NAO index over the ten day analysis period of each case study. The daily and the ten day indices are shown on Figure 5 (red and blue bars and orange and blue lines, respectively). The comparison between the ten day NAO index and the monthly NAO index revealed that the first would allow a more accurate classification of each case study as a positive or negative NAO index storm (Table 3 and Figure 5). The monthly NAO index for cases 3 and 7, which overlap two consecutive months, December 1998 and January 1999 and October and November 2003 respectively, was averaged between the two months. The monthly NAO index phase didn’t agree with the ten day NAO index in case studies 1, 4, 5 and 7 listed in Table 2.

The analysis of the synoptic background behind each storm, revealed, with no exception, that in all the cases there were several low pressure systems that evolved over the North Atlantic, during the analysis period. It has been known for several decades that the East coast of the United States (US), from Florida to the Carolinas, is highly cyclogenetic (Miller, 1946), mainly during the winter season.

Case	Monthly NAO index	10 day NAO index	Storm classification
1	-0.7260	0.6634	Positive
2	-0.8394	-1.5953	Negative
3	0.5405	0.5155	Positive
4	0.3954	-0.4441	Negative
5	0.1008	-0.7115	Negative
6	-0.9202	-1.261	Negative
7	-1.708	0.9718	Positive

Table 3. Storm classification in accordance with the ten day NAO index phase.

In fact the western side of the Atlantic Ocean is one of the principal sites for cyclone development, due to the strong sea-surface temperature gradient (Carlson, 1994). Cyclones can also develop south of Greenland, over the North Atlantic Ocean. These storms have an associated frontal system that in turn aids the formation of new cyclones, and gives rise to storm trains across the North Atlantic. In fact this idea was already contained in Bjerknes and Solberg’s (1922) historical description of the cyclone family which required a ‘mother’ cyclone to

initiate the wave developments leading to secondary low pressure systems and sea level cut-off lows. There is a clear relationship between the cyclogenetic processes in the North Atlantic and the NAO: positive NAO index situations favor the formation of deep primary low pressure systems and secondary lows along their frontal zones, and tend to contribute to a higher number of storms in the North Atlantic basin. To establish a link between the storm track of individual cyclone and the NAO index, the low pressure centers responsible for the formation of each storm wave event were tracked from their genesis to occlusion and plotted on a map.

C. CASE ANALYSIS

1. Case I – February 1 to 10, 1994 (Positive)

The ten day analysis period for case 1, from February 1 to February 10, was characterized by a positive ten day NAO index (Figure 5). On 01/00Z a secondary low developed a few hundred miles northwest of the Azores, about 45°N, and quickly deepened to 959 hpa. This low tracked northeast and occluded west of Ireland on 05/06Z (Figure 6). Between 02/18Z and 04/12Z, winds at the surface of this low were oriented towards the Iberian Peninsula, with a maximum at 03/00Z and surface wind speeds in excess of 65 knots (Figure 7). These northwesterly winds provided a favorable two day long fetch that would impact Portugal, generating extremely high waves. This storm lasted 57 hours and 10 minutes (from 03/0620Z to 05/1530Z), and was most intense at buoy P1.

The wave parameters measured at the four buoys are indicated in Table 4. Figures 8 and 9 show the time history evolution of the wave parameters during this event. The

highest waves were observed at buoy P1, ranging from 5 to 9 meters over a 57 hours period. At buoy P2 the wave heights were about 20 percent smaller. The peak period was relatively long at buoys P1 and P2 (~18 seconds), indicative of a swell dominated event. At buoys P3 and P4 the peak period during the storm was shorter. The maximum peak period at buoy P3 occurred several days after the peak of the storm. The peak wave direction was northwesterly at buoys P1 and P2 and consistent with the wind direction in the generation region shown in Figure 7. The relatively narrow spread suggests a concentration of swell on a narrow swath. The peak wave direction at buoy P3 was southwesterly, which is consistent with the expected coastal sheltering at this site. The energy spectra (frequency spectra at the time of the maximum significant wave height) confirm the strong swell dominance at buoys P1 and P2, with a sharp peak at lower frequencies. At buoys P3 and P4 the energy was spread more evenly over the frequency spectrum, indicative of the importance of the wind sea at these locations (Figure 9). There was no directional data available at buoy P4 for this case study.

2. Case II – 21 to 30 November 1997 (Negative)

The ten days NAO index for case 2, from November 21 to 30, was negative (Figure 5). During this period several lows crossed the North Atlantic basin; from the east coast of the US, southwest toward Europe, exhibiting a considerable meridional width. On 22/18Z a new mid-latitude cyclone started to develop, off the shore of North Carolina, at about 35°N. This low tracked east and occluded in northern Spain at 26/06Z (Figure 10). Between 24/06Z and 26/00Z, this low exhibited strong westerly winds that were

oriented toward the west coast of Portugal and Spain, with a maximum at 24/18Z, and having winds at the surface in excess of 55 knots (Figure 11). These westerly winds provided a favorable fetch that would be responsible for the extremely high waves measured in Portugal at this time. This storm was active from 24/03Z to 26/0956Z (54 hours and 56 minutes) off the coast of Portugal, and was most intense at buoy P2.

The wave parameters measured at buoys P1 to P4 are given in Table 4. Figures 12 and 13 show the evolution of the wave parameters during this event. The early significant wave height maxima at buoys P1 and P2 with relatively long periods (20 seconds) are indicative of old swell from a previous storm. Shorter peak periods at these buoys (15-16 seconds) were observed at the height of the storm. This fact is coincident with the storm track, towards the Iberian Peninsula. The shorter periods are indicative of younger swell generated as the storm tracked between the Azores and Portugal’s main land. The significant wave height at buoys P3 was the highest of all case studies. The maximum peak period at this buoy occurred several days after the peak of the storm. The peak wave direction was west-northwest at buoys P1 and P2. The more westerly directions at higher frequencies (Figure 13) suggests that these waves were generated later as the storm tracked towards the Iberian Peninsula. The peak wave direction at buoys P3 was close to west-southwest, and close to west at buoy P4. The energy spectra were similar to case 1: narrow at buoys P1 and P2 and broader at buoys P3 and P4.

3. Case III – 25 December 1998 to 3 January 1999 (Positive)

Case study 3, with an analysis period from December 25 to January 3 was characterized by a positive ten day NAO index (Figure 5). On 27/06, off the shore of New England, a mid-latitude cyclone developed, quickly deepening to 969 hpa. This low tracked northeast and occluded in the North Sea on 01/00Z (Figure 14). Between 28/06Z and 29/12Z, this low exhibited winds at the surface level that were oriented toward the Iberian Peninsula (with a maximum at 28/06Z) with speeds higher than 70 knots (Figure 15). These west-northwesterly winds provided a favorable fetch that generated extremely high waves off the shore of Portugal. The storm in this case study was more intense at buoy P1 (Figures 16 and 17) and lasted 38 hours and 50 minutes, from 29/0942Z to 31/0032Z.

The wave parameters registered at the four buoys are shown in Table 4, and Figures 16 and 17. The significant wave height evolution at buoy P1 and P2 is similar with maxima of 8.8 and 7.95 meters respectively and corresponding peak periods of about 18 seconds. Longer peak periods were observed at these two buoys several days before the storm, indicative of the presence of old swell from a distant storm. The significant wave height maxima at buoys P3 and P4 occurred after the storm ended, with peak directions suggesting a more southerly source. The peak wave direction was west-northwest at buoy P1 and more northwesterly at buoy P2. The presence of energy at higher frequencies at buoy P1 prior to the peak of the storm is indicative of local generation by strong winds passing through this buoy’s site (Figure 17). The directional

spread was narrow (less than 20 degrees) at buoys P1 to P3. Buoy P4 had a more variable incoming swell direction prior to the storm, on 27 and 28 December, which resulted in a 45° spread. The energy spectra behavior was similar to the previous cases.

4. Case IV – October 18 to 28, 1999 (Negative)

The ten day analysis period for case 4, from October 18 to 28, was characterized by a negative ten day NAO index (Figure 5). On 14/00Z a tropical storm developed in the Caribbean, south of Cuba. The low tracked northeast toward the east coast of the US and transitioned into a mid-latitude cyclone. This low intensified as it tracked northeast, to the east coast of North America first, until about 50°N, and then southeast, toward the Biscay Gulf, where it occluded at 21/12Z (Figure 18). From 19/18Z to 22/18/Z the surface winds associated with this low were oriented southwest, toward the Iberian Peninsula, with a maximum at 20/06Z, with wind speeds in excess of 70 knots (Figure 19). These northwesterly winds provided a favorable fetch that would impact Portugal, generating extremely high waves. This storm lasted 49 hours and 16 minutes, from 22/0206Z to 24/0333.

The wave parameters measured at the four buoys are shown in Table 4 and Figures 20 and 21. The significant wave height was higher at buoy P1, with a single maximum. At buoy P2 the significant wave height time series shows a double peak. The peak period maxima at these two buoys coincided with the beginning of the storm (~20 seconds), indicating the dispersive arrivals of the north-westerly swell. The maximum significant wave height at buoy P3 occurred several days before the storm. At buoy P4 the

significant wave height maximum occurred a few hours before to the storm started to affect buoy P1. In both cases this maxima are related to old swell. The peak wave direction was consistently northwest at buoys P1 and P2. The spread was relatively low at all four buoys.

5. Case V – January 19 to 28, 2002 (Negative)

Case 5 was characterized by a negative ten day NAO index (Figure 5) during the analysis period, from January 19 to 28. A bomb-type, mid-latitude cyclone formed at 20/00Z, off the shore of North Carolina, quickly deepening to 957 hpa. It tracked east toward the Azores, then east-northeast toward the Biscay Gulf, and occluded in the south of England (Figure 22) at 23/12Z. From 23/09Z to 24/1235Z this low exhibited east oriented winds at the surface toward the west coast of Portugal, with a maximum at 22/00Z, with wind speeds higher than 70 knots (Figure 23). These westerly winds provided a favorable fetch that generated extremely high waves off the Portugal shore. This storm lasted from 23/09Z to 24/1235Z (27 hours and 35 minutes), and was most intense at buoy P1.

The wave parameters are shown in Table 4 and Figures 24 and 25. The significant wave height time series of buoys P1 and P2 show only a single peak, which is indicative of a single event. The significant wave height was higher at buoy P1. The maximum peak period was relatively long at buoys P1 and P2 (~20 seconds) and coincided with the storm peak time. The significant wave height time series at buoy P3 had a behavior similar to buoys P1 and P2 but was considerably lower (2.64 meters). The peak period at this buoy was also lower, but the maximum occurred several days before the storm. The peak wave direction was west-

northwest at buoys P1 and P2 and west-southwest at buoy P3. These differences indicate that the dominant long period waves observed at buoys P1 and P2 were blocked by the southwest tip of Portugal and did not reach buoy P3.

6. Case VI – December 22 to 31, 2002 (Negative)

Case 6 took place from December 22 to 31 and was characterized by a negative ten day NAO index (Figure 5). A mid-latitude cyclone started to develop west of the Azores at 25/12Z, and deepened to 979 hpa. This low tracked east toward the Azores and then northeast, toward the Biscay Gulf, where it occluded at 27/00Z (Figure 26). Between 26/00Z and 26/18Z, this low exhibited surface winds oriented east toward the west coast of Portugal, with a maximum at 26/06Z, with wind speeds at the surface higher than 55 knots (Figure 27). These westerly winds provided a favorable fetch that impacted Portugal by generating extremely high waves. The storm lasted 49 hours and 57 minutes (from 26/0340Z to 27/1027Z) and was most intense at buoy P2.

The wave parameters are shown in Table 4 and Figures 28 and 29. As in case 4, the significant wave height time series at buoys P1 and P2 are indicative of a single event. The significant wave height was highest at buoy P2 (8.21 meters) and relatively low at buoys P3 and P4. The maximum peak period at buoys P1 and P2 was shorter than in the previous cases (~17 seconds) and coincided with the storm peak. The maximum significant wave height at buoy P4 occurred more than two days before the storm was felt at buoy P1. The peak wave direction was west at buoy P1, close to west at buoy P2 and west-southwest at buoy P3. The

distribution of energy over the frequency spectrum at buoy P3 is indicative of a strong wind wave component at this buoy.

7. Case VII – October 27 to November 5, 2003 (Positive)

The ten day analysis period for case 7, from October 27 to November 5, was characterized by a positive ten day NAO index (Figure 5). On 28/00Z, a mid-latitude cyclone started developing over New England. This low tracked northeast toward Greenland, and then east-northeast, toward the British Islands, and occluded over the Biscay Gulf at 01/06Z (Figure 30). Between 29/18Z and 31/06Z, this low exhibited surface winds oriented toward the Iberian Peninsula, with a maximum at 30/00Z, with surface wind speeds in excess of 60 knots (Figure 31). These northwesterly winds provided a fetch that impacted the west coast of Portugal and the north and west coasts of Spain, generating extremely high waves in these locations. This storm lasted from 30/1922Z to 01/1616Z (44 hours and 54 minutes), and was most intense at buoy P1.

The wave parameters are shown in Table 4 and Figures 32 and 33. The significant wave height grew rapidly at buoy P1, where it was higher than at the other buoys. The peak period maxima were similar at the four buoys (~18 seconds), and occurred during the storm at buoys P1 and P2, but a few days earlier at buoy P4. The significant wave height at buoys P3 and P4 followed about the same pattern as at buoys P1 and P2. The peak wave direction was northwest at buoys P1 and P2, west-southwest at buoy P3 and close to west at

buoy P4. The spread was narrow at buoys P1 to P3 but broad at buoy P4, suggesting the presence of swell from a different source.

	Buoy	Storm duration (Hr)	Maximum significant wave height (m)	Peak period (s)	Peak wave direction
Case 1 (positive)	P1	57:10	8.76	16.7	318
	P2	32:00	6.42	16.7	312
	P3	-	2.62	6.9	255
	P4	-	1.48	9.1	NA
Case 2 (negative)	P1	54:56	6.27	16.7	298
	P2	51:56	7.65	15.4	286
	P3	-	4.1	10	257
	P4	-	2.81	7.7	285
Case 3 (positive)	P1	38:50	8.8	18.2	286
	P2	34:36	7.95	18.2	295
	P3	-	3.89	6.9	219
	P4	-	2.51	7.4	283
Case 4 (negative)	P1	49:16	7.81	16.7	295
	P2	31:32	7.14	18.2	303
	P3	-	4.01	8.7	261
	P4	-	2.27	6.7	265
Case 5 (negative)	P1	27:35	7.72	18.2	281
	P2	22:39	7.24	18.2	298
	P3	-	2.64	7.1	231
	P4	-	-	-	-
Case 6 (negative)	P1	49:57	7.71	15.4	268
	P2	22:41	8.21	15.4	288
	P3	-	3.96	8	248
	P4	-	2.99	15.4	275
Case 7 (positive)	P1	44:54	9.7	16.7	311
	P2	16:29	6.59	16.7	308
	P3	-	3.2	7.1	260
	P4	-	1.52	6.6	280

Table 4. Wave parameters and storm durations of the seven case studies.

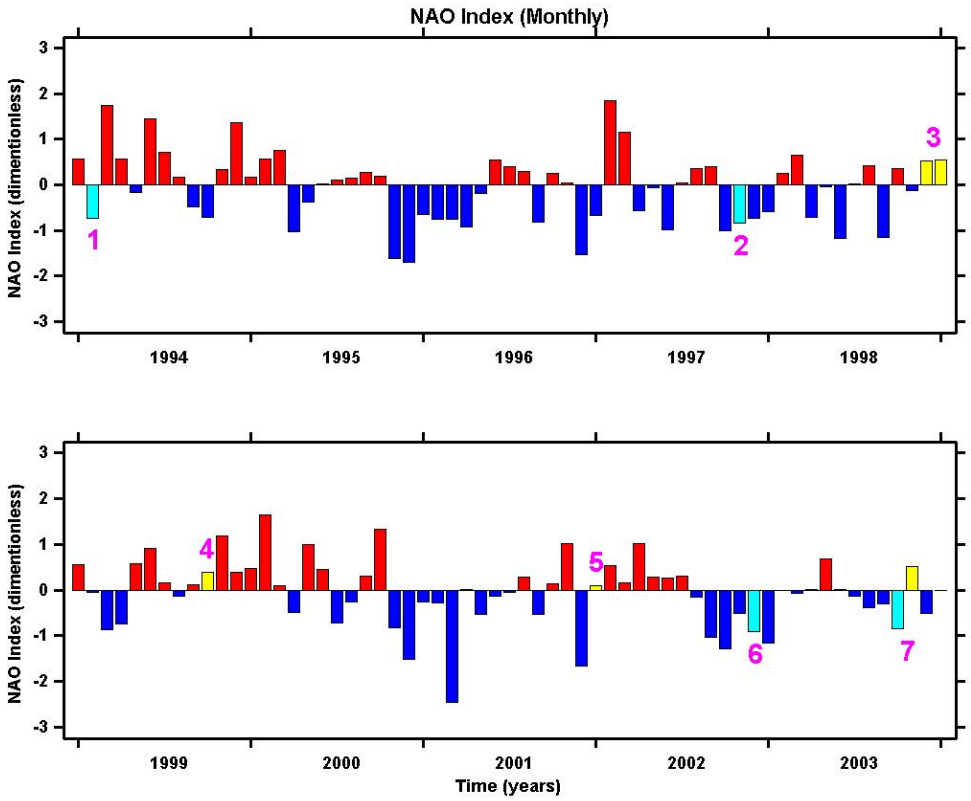

Figure 4. Monthly NAO index from 1994 to 2003.

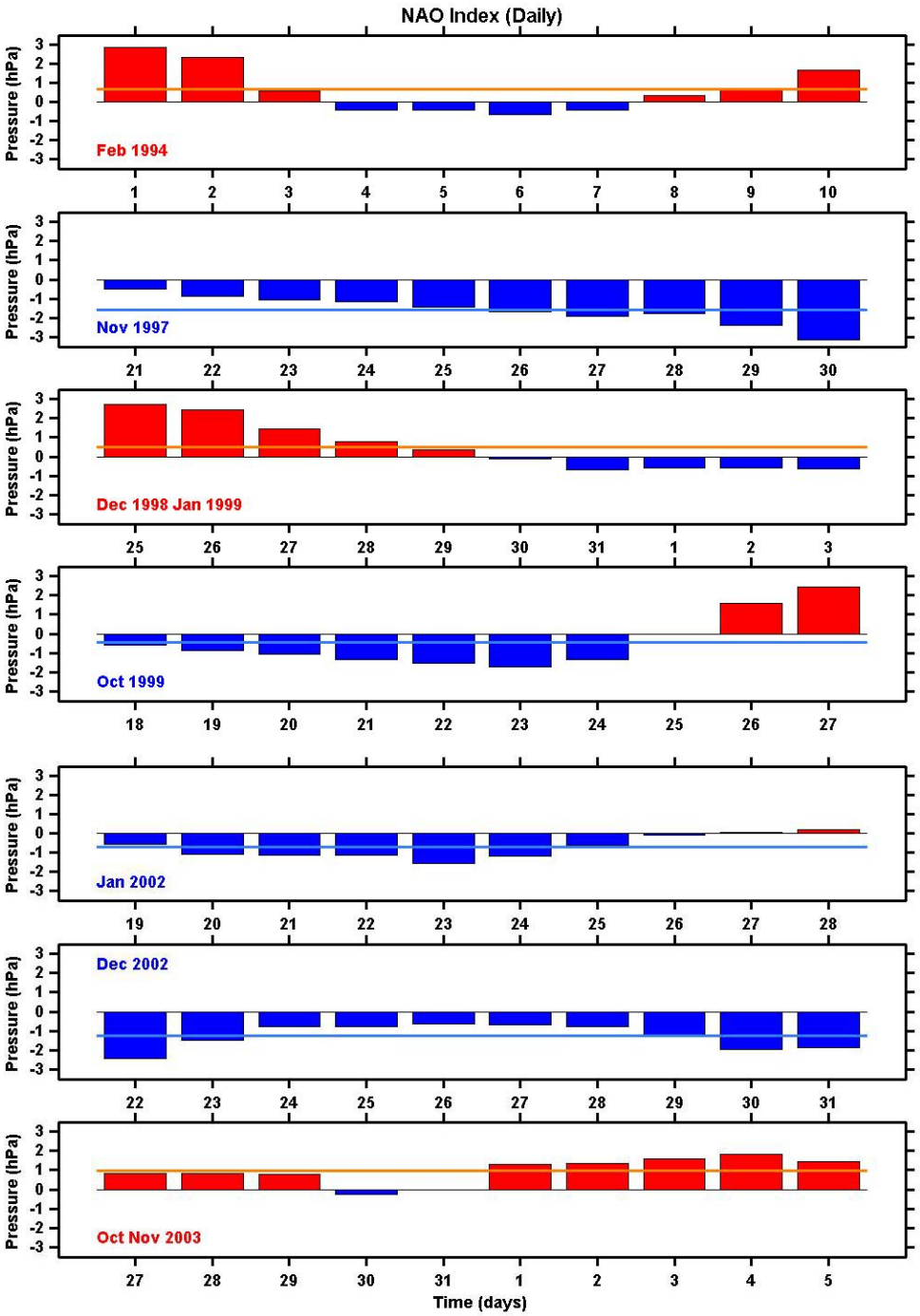

Figure 5. Daily (red and blue bars) and ten day NAO index (orange and light blue lines) for the seven case studies.

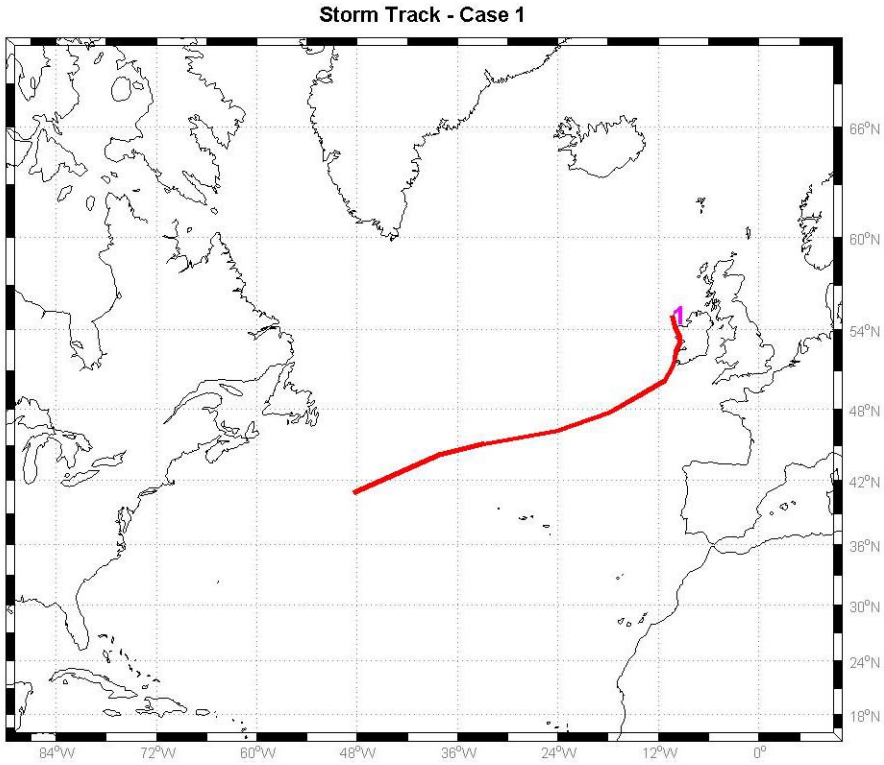

Figure 6. Case 1 – storm track from 01/00Z to 05/06Z.

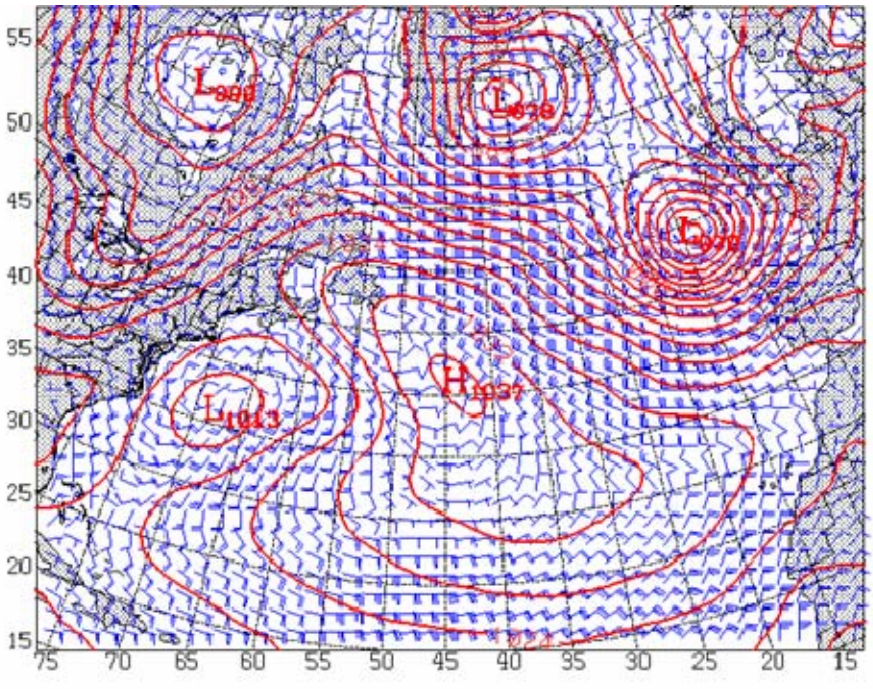

Figure 7. Case 1 – synoptic picture at 03/00Z.

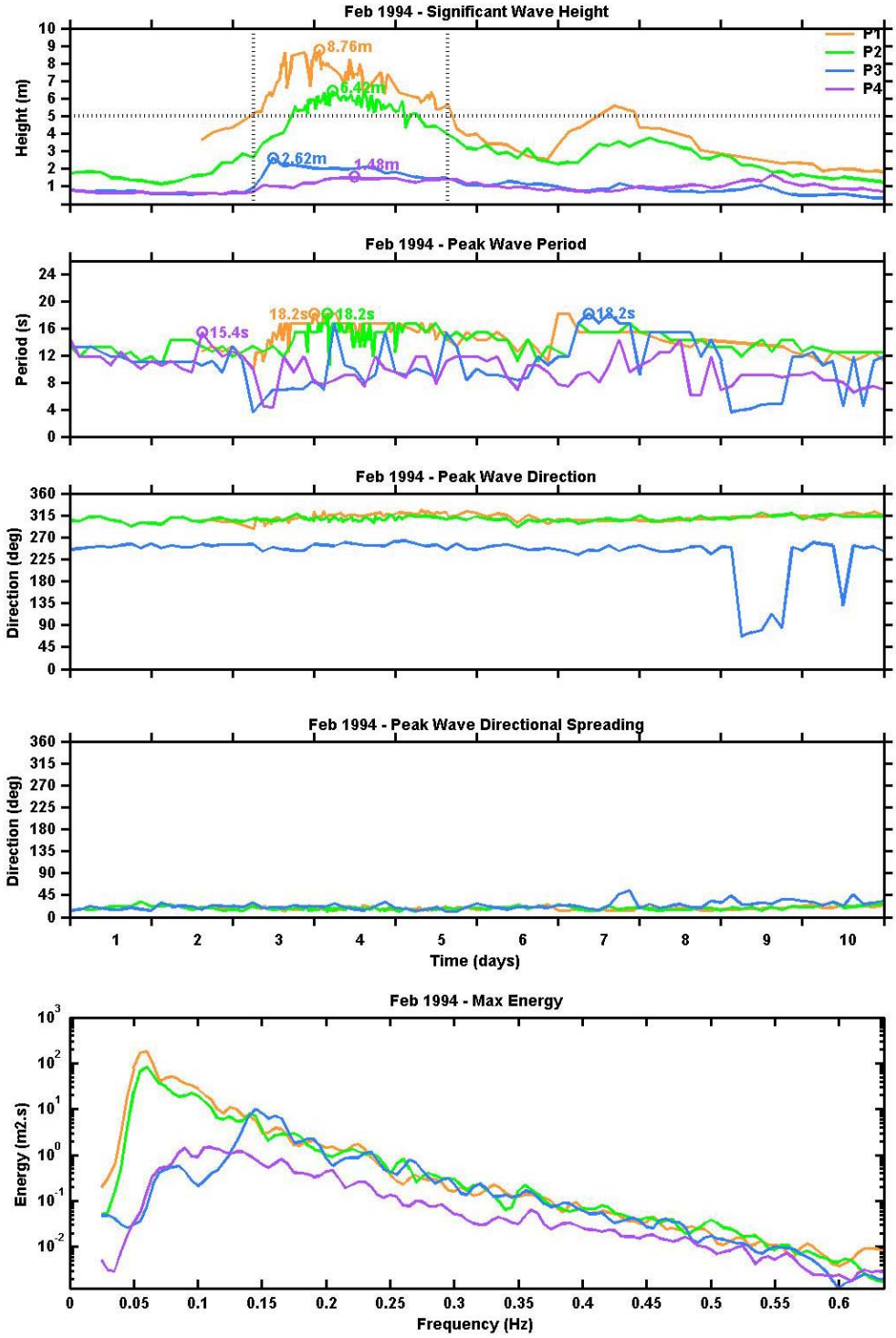

Figure 8. Case 1 - wave parameters.

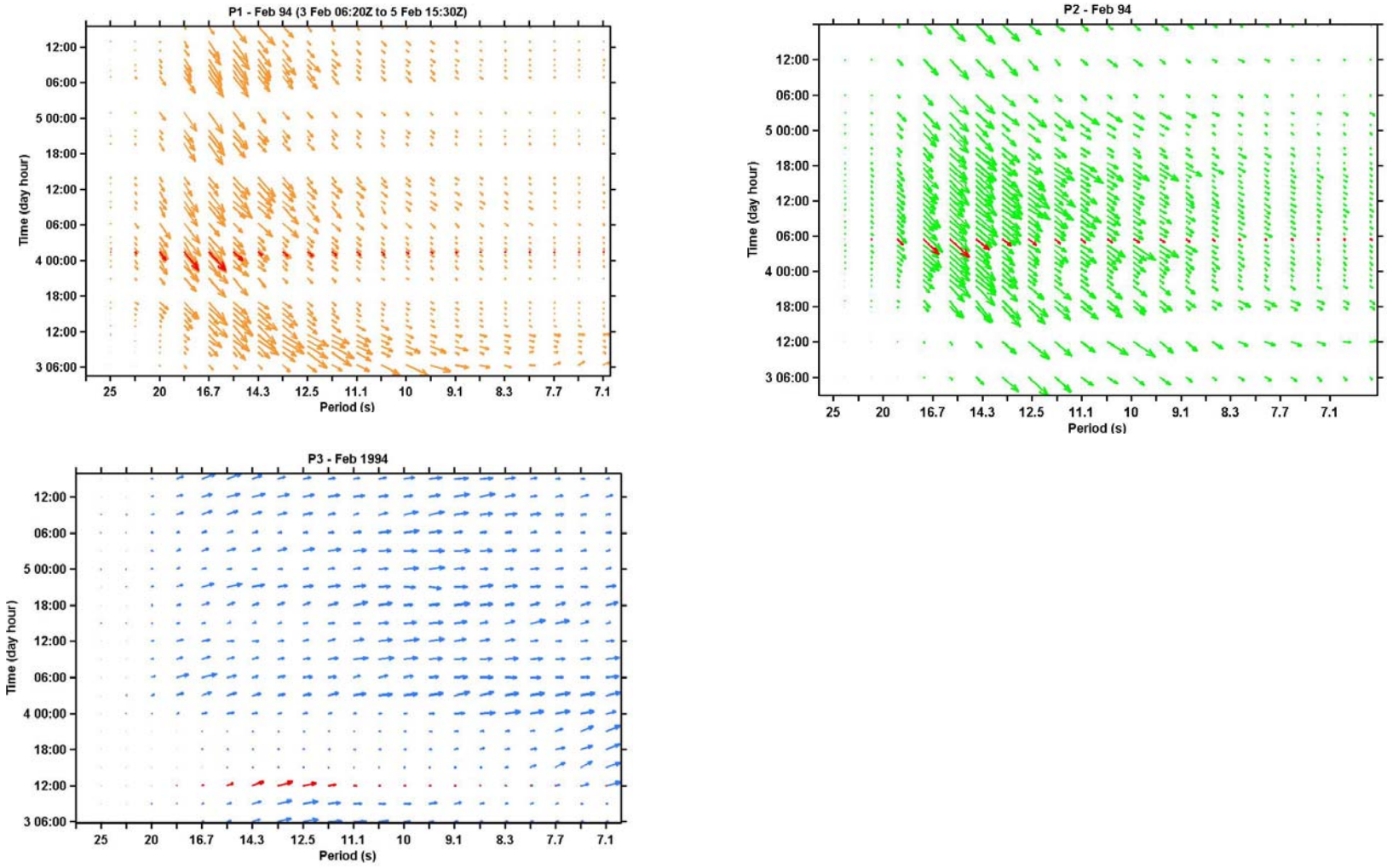

Figure 9. Evolution of energy density (arrow length logarithmically scaled) and mean direction (at each frequency) during storm case 1. Time of maximum energy indicated in red.

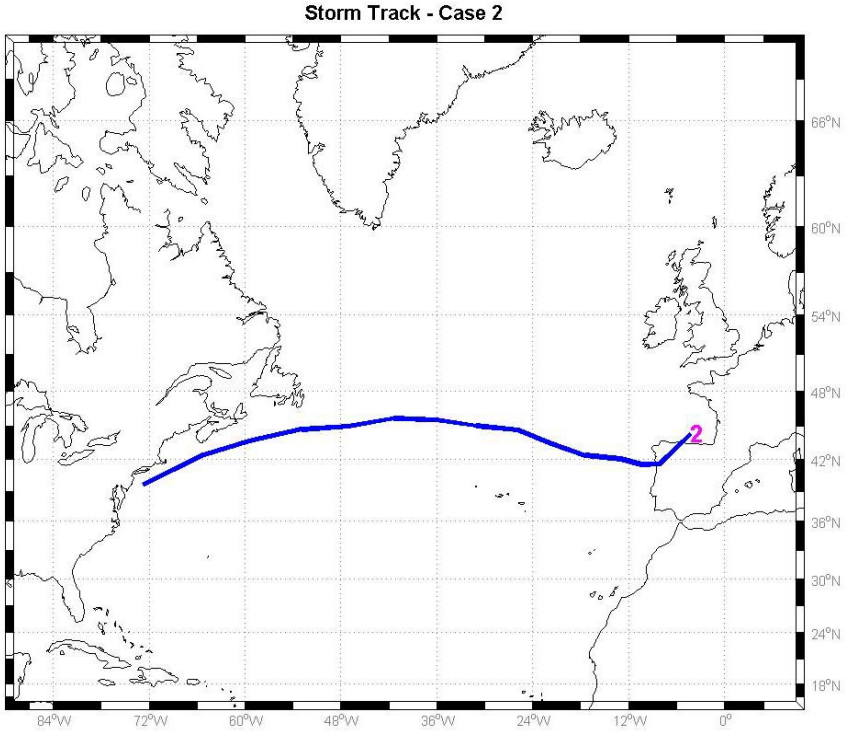

Figure 10. Case 2 – storm track from 22/18Z to 26/06Z.

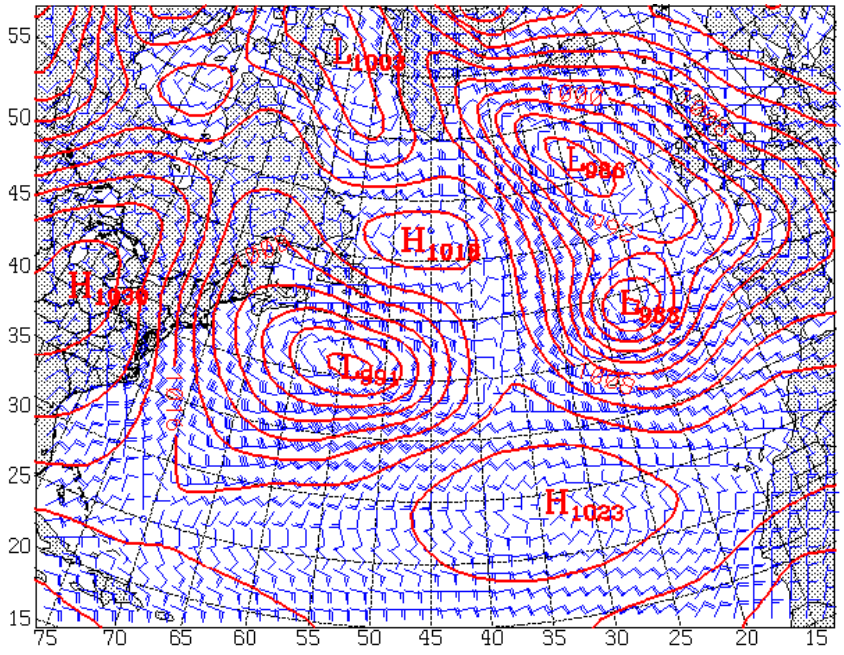

Figure 11. Case 2 – Synoptic picture at 24/18Z.

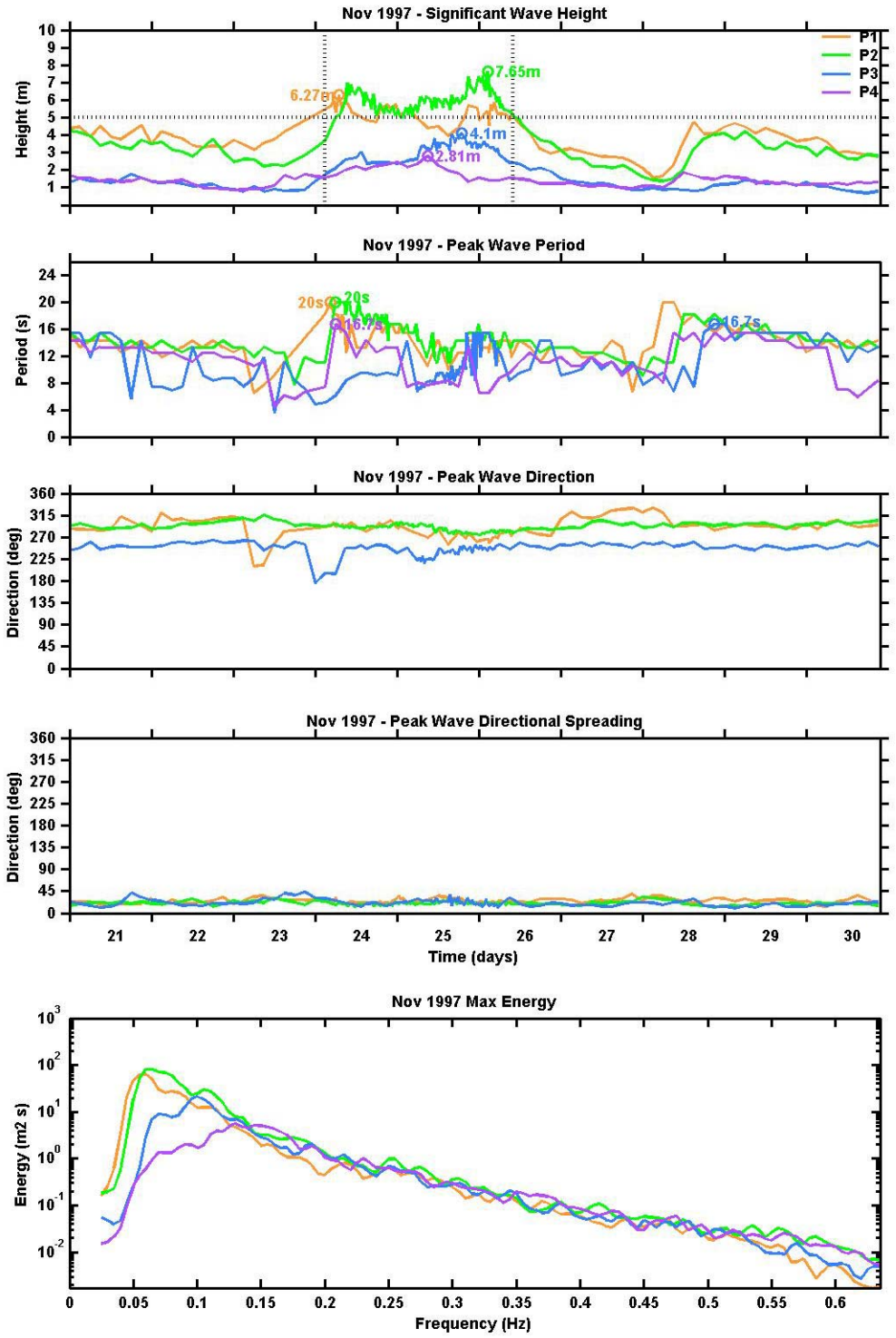

Figure 12. Case 2 - wave parameters.

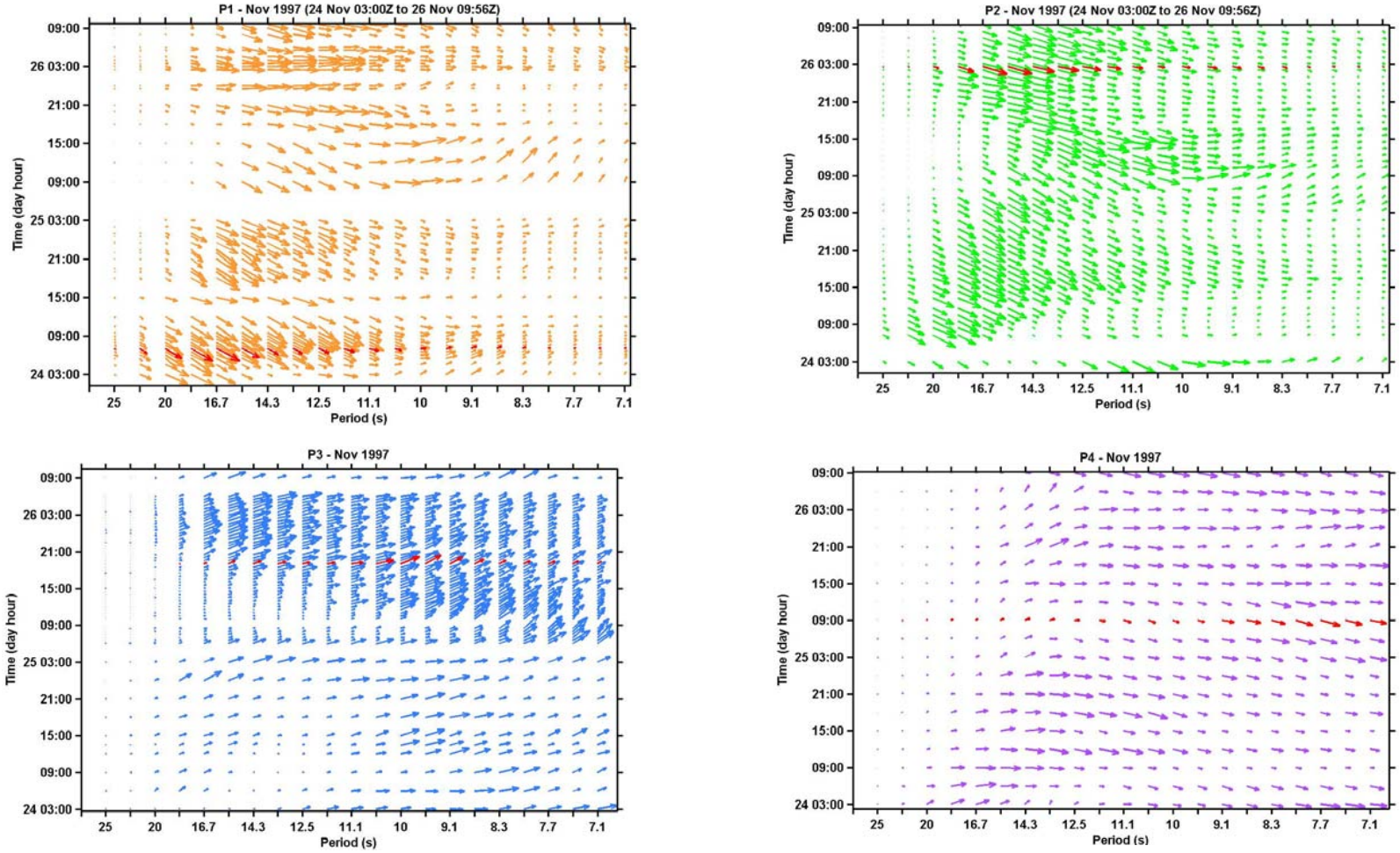

Figure 13. Evolution of energy density (arrow length logarithmically scaled) and mean direction (at each frequency) during storm case 2. Time of maximum energy indicated in red.

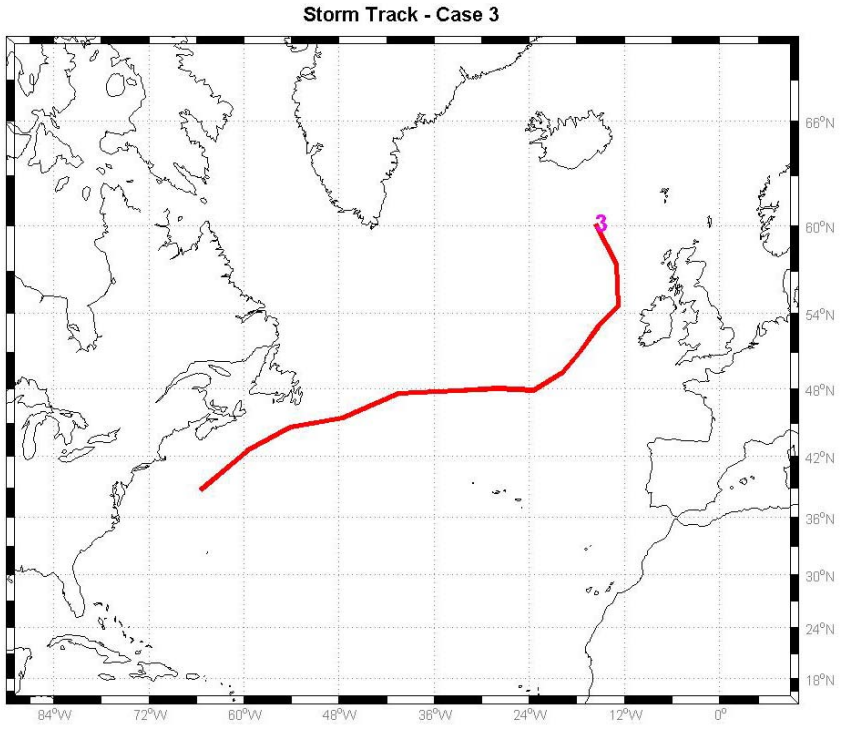

Figure 14. Case 3 – Storm track from 27/06Z to 01/00Z.

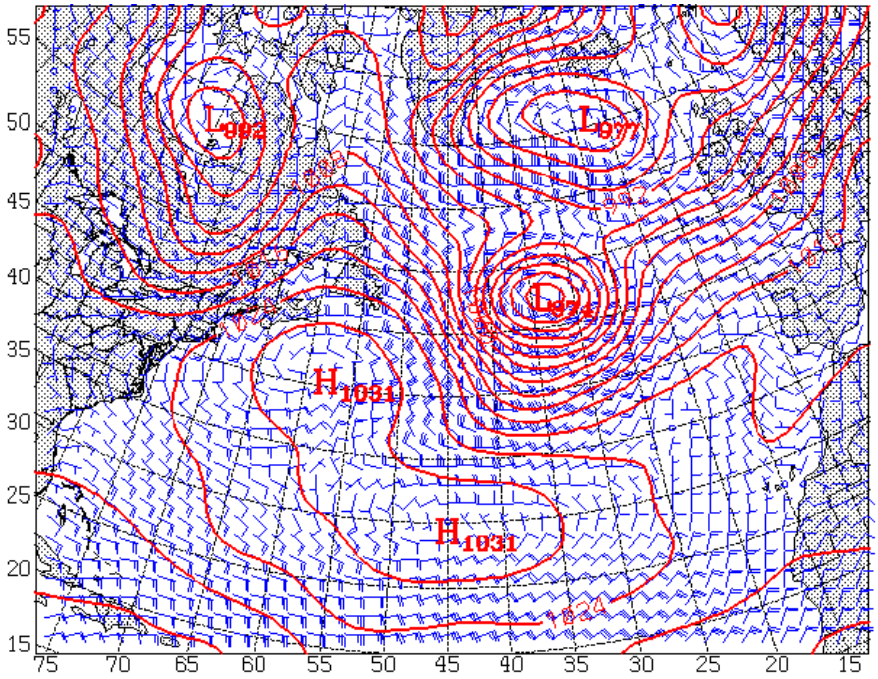

Figure 15. Case 3 – synoptic picture at 28/06.

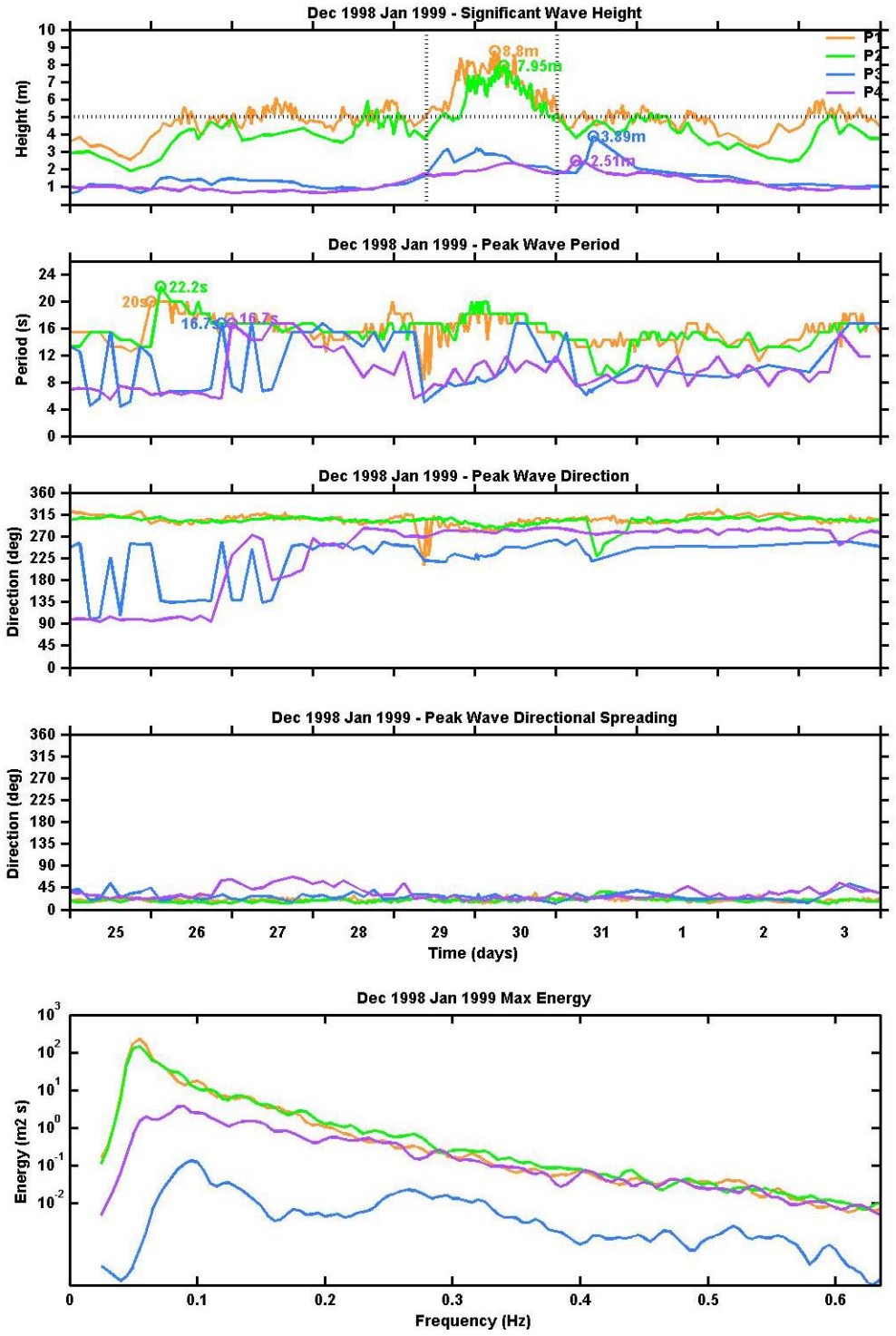

Figure 16. Case 3 - wave parameters.

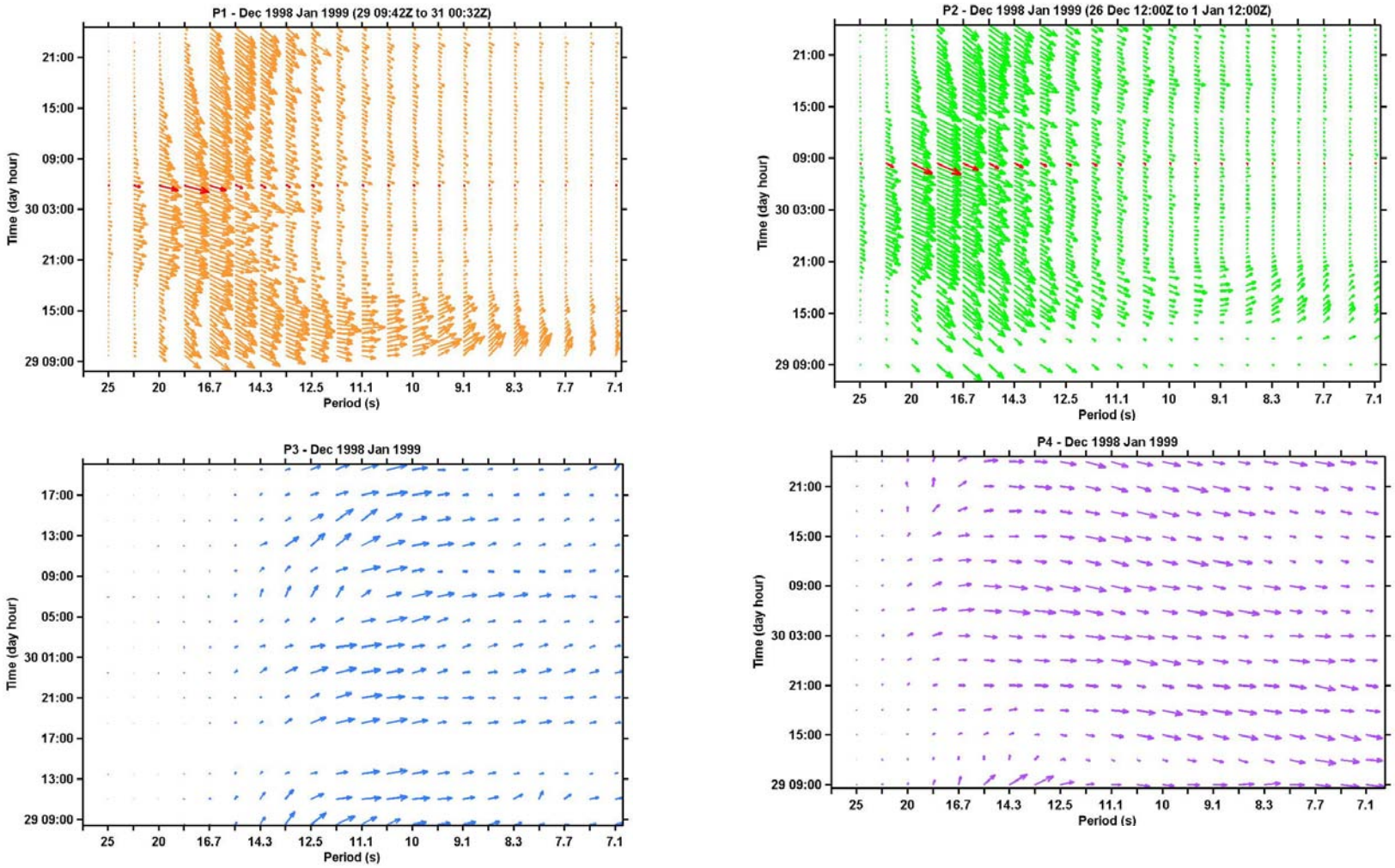

Figure 17. Evolution of energy density (arrow length logarithmically scaled) and mean direction (at each frequency) during storm case 3. Time of maximum energy indicated in red.

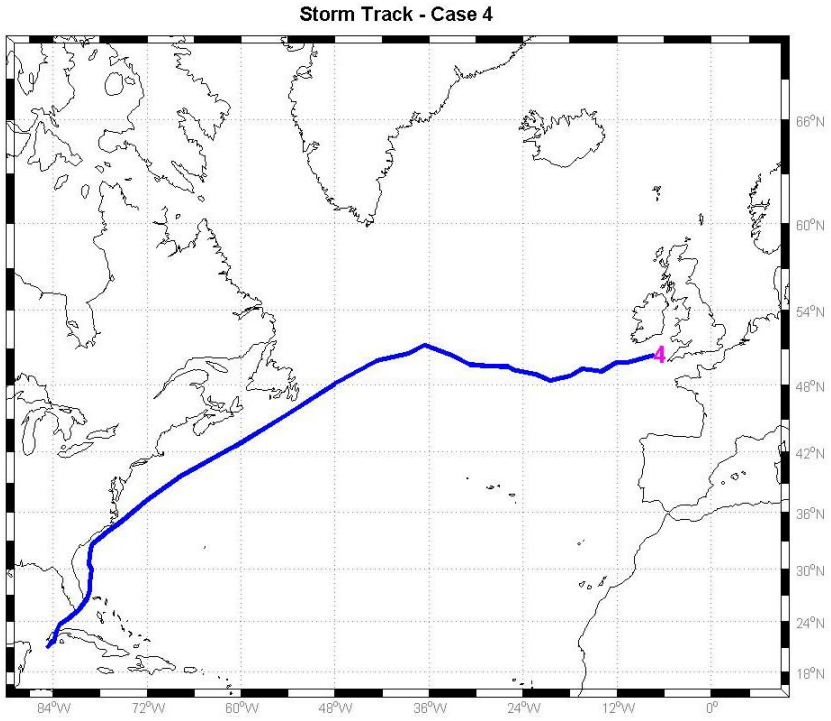

Figure 18. Case 4 – storm track from 14/00Z to 24/1200Z (extratropical transition).

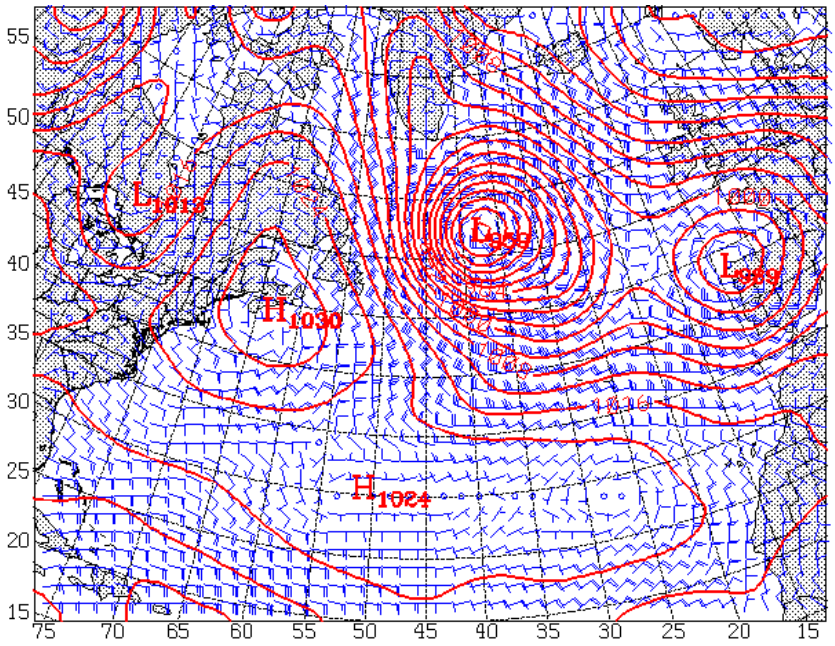

Figure 19. Case 4 – synoptic picture at 20/06.

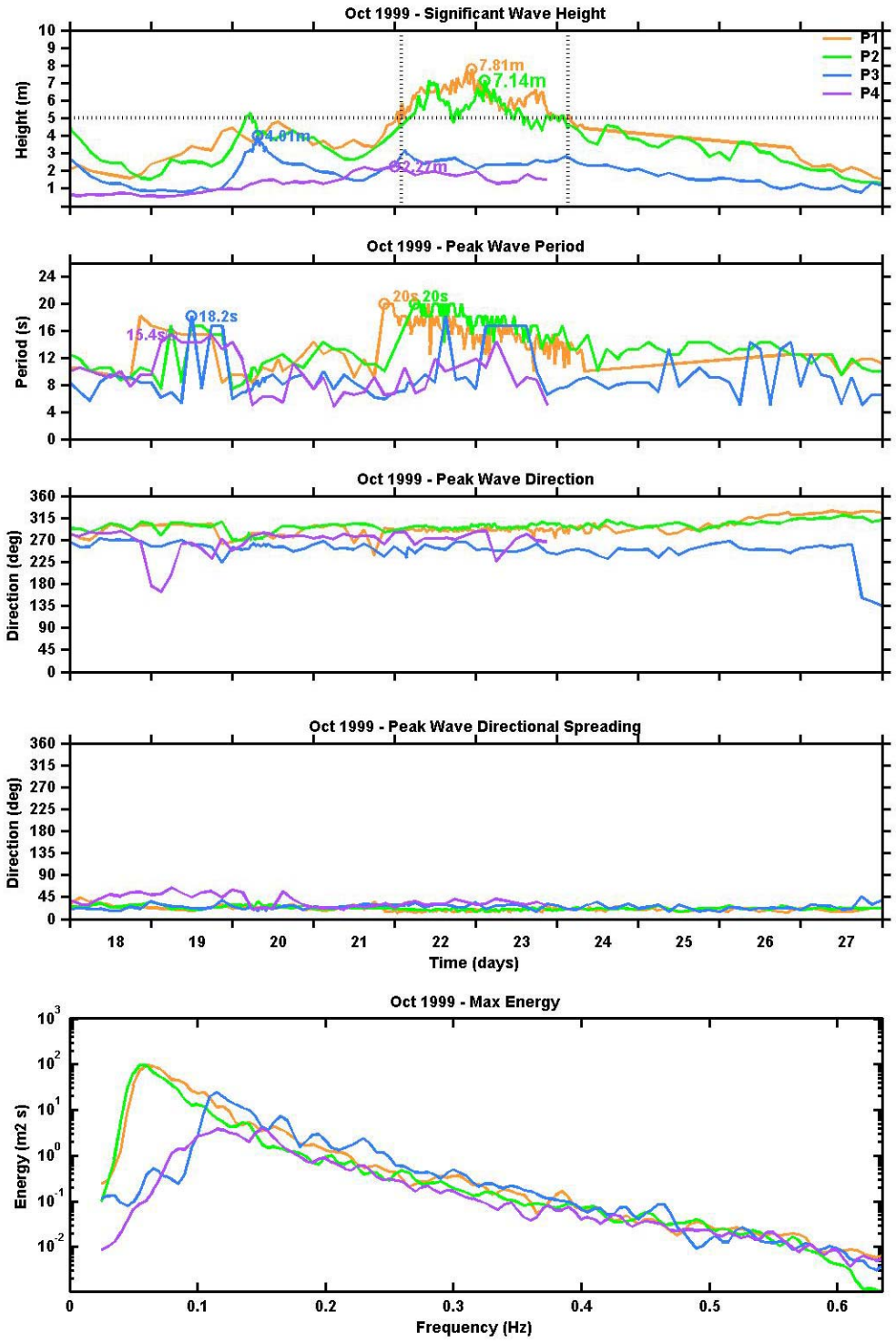

Figure 20. Case 4 - wave parameters.

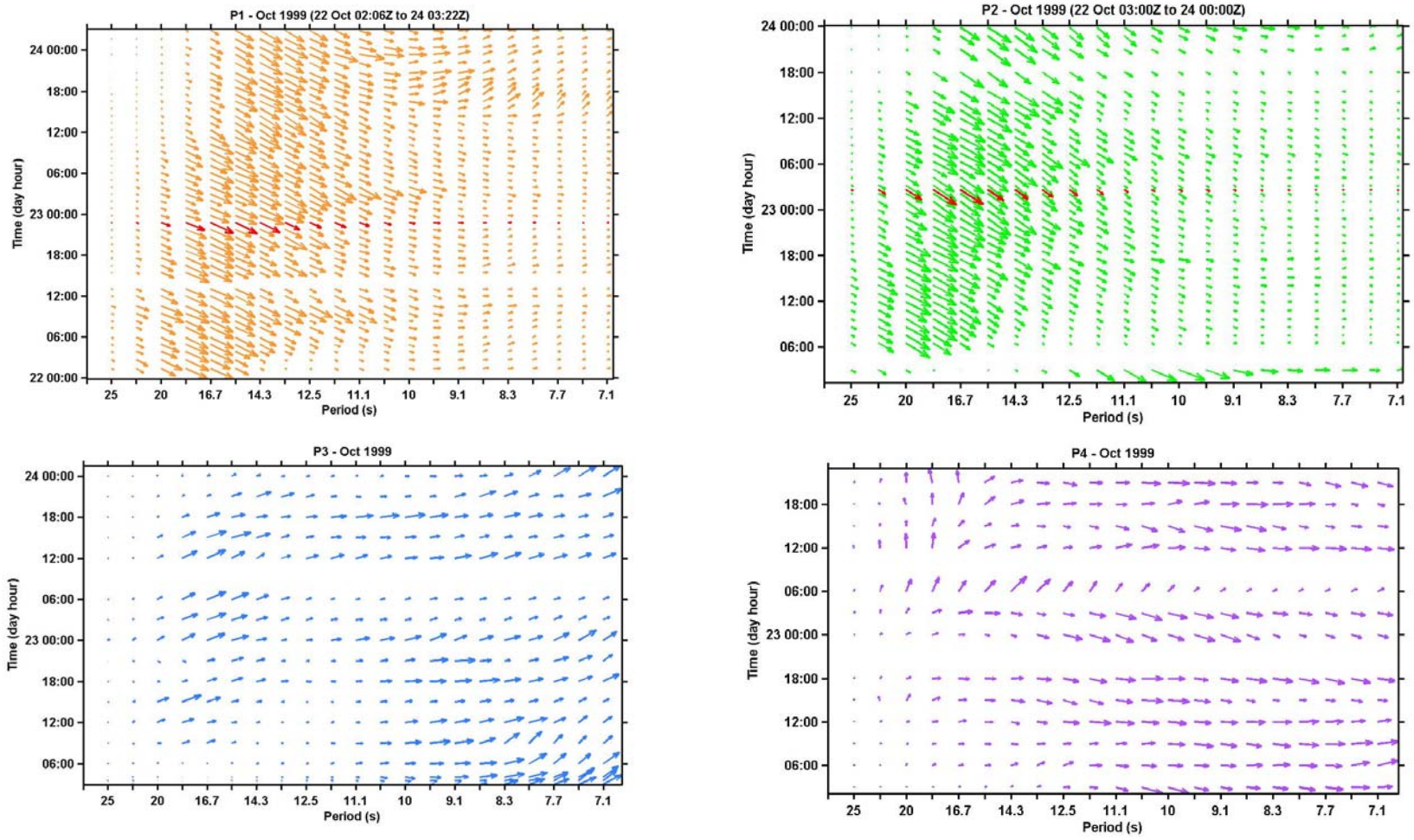

Figure 21. Evolution of energy density (arrow length logarithmically scaled) and mean direction (at each frequency) during storm case 4. Time of maximum energy indicated in red.

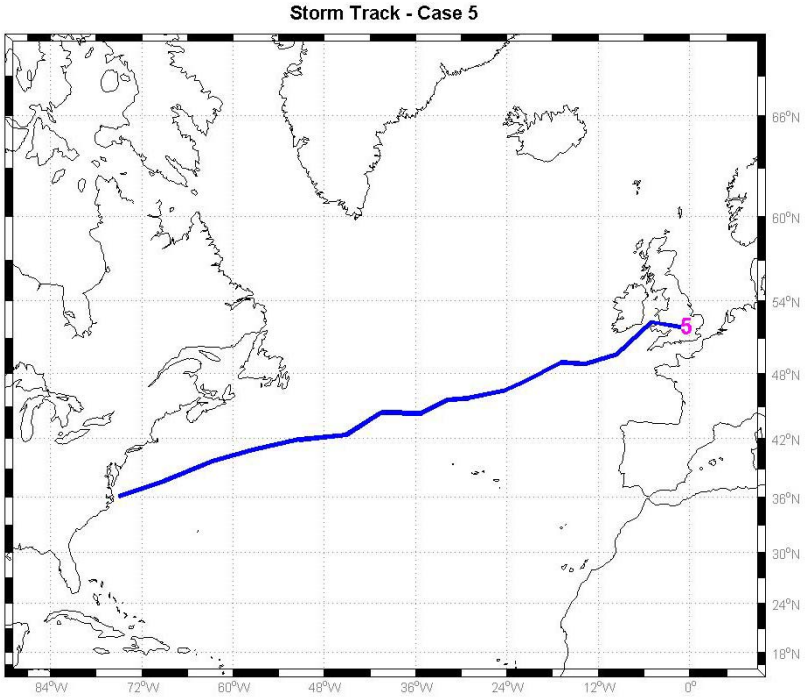

Figure 22. Case 5 – storm track from 20/00Z to 23/12Z.

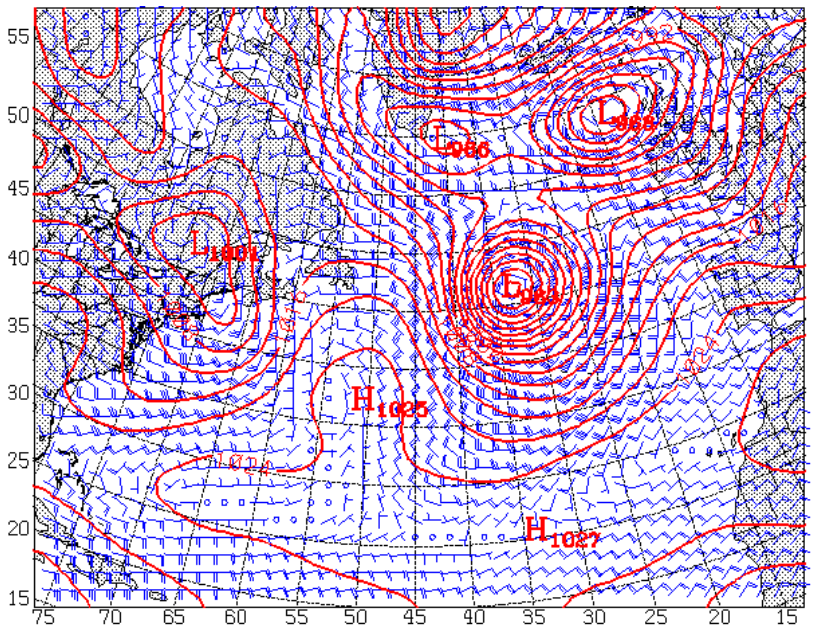

Figure 23. Case 5 – synoptic picture at 22/00Z.

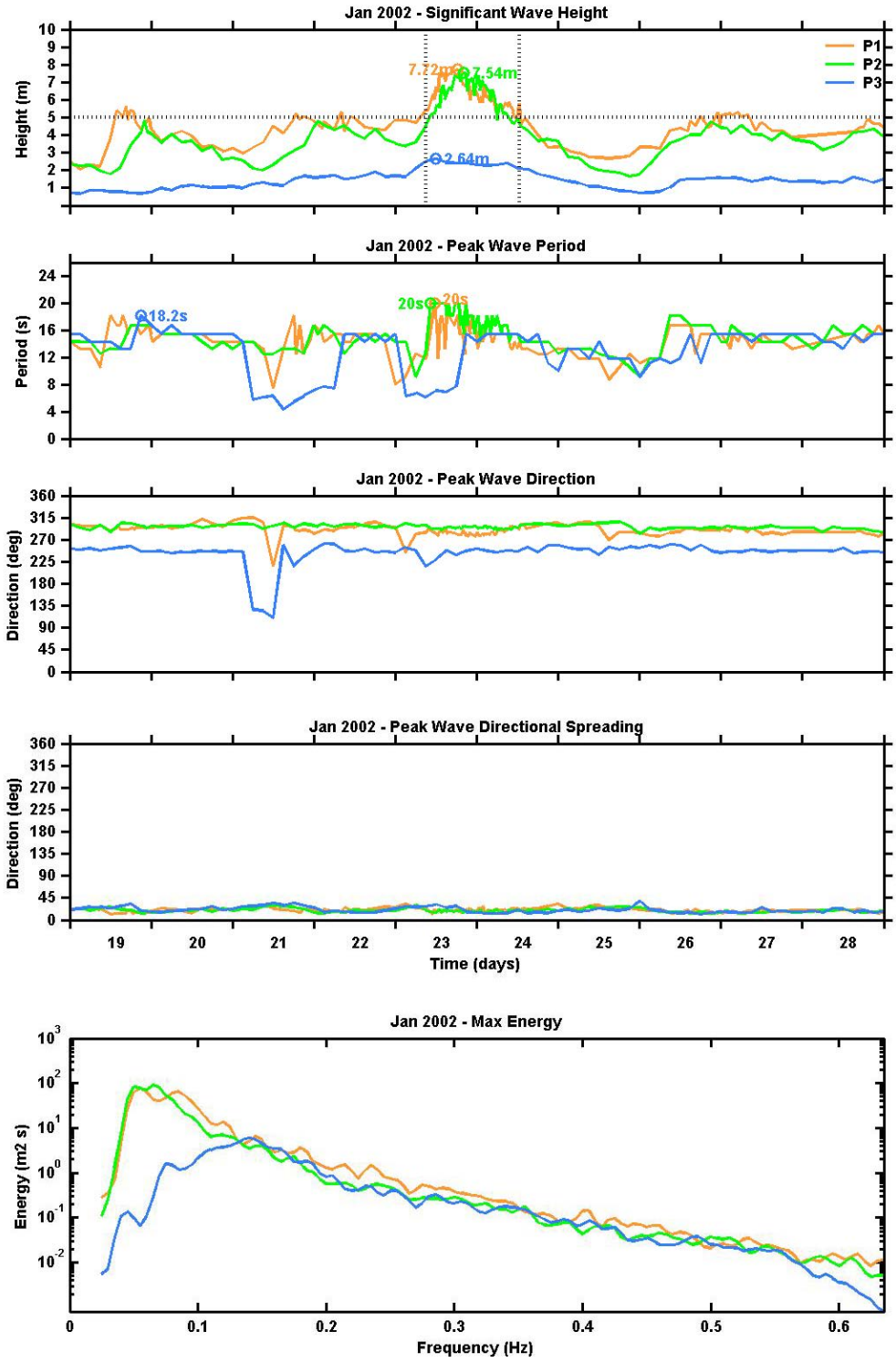

Figure 24. Case 5 – wave parameters.

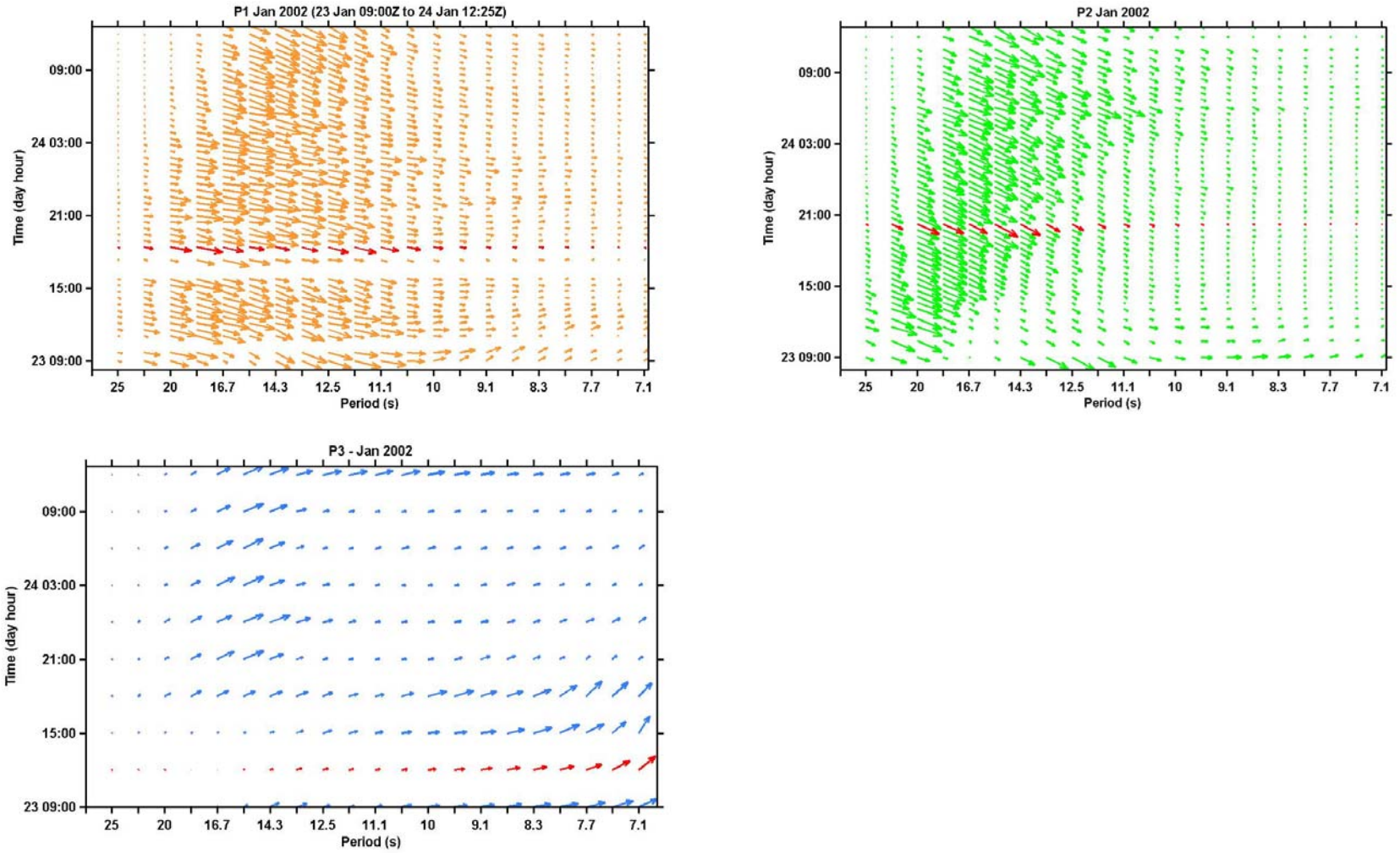

Figure 25. Evolution of energy density (arrow length logarithmically scaled) and mean direction (at each frequency) during storm case 5. Time of maximum energy indicated in red.

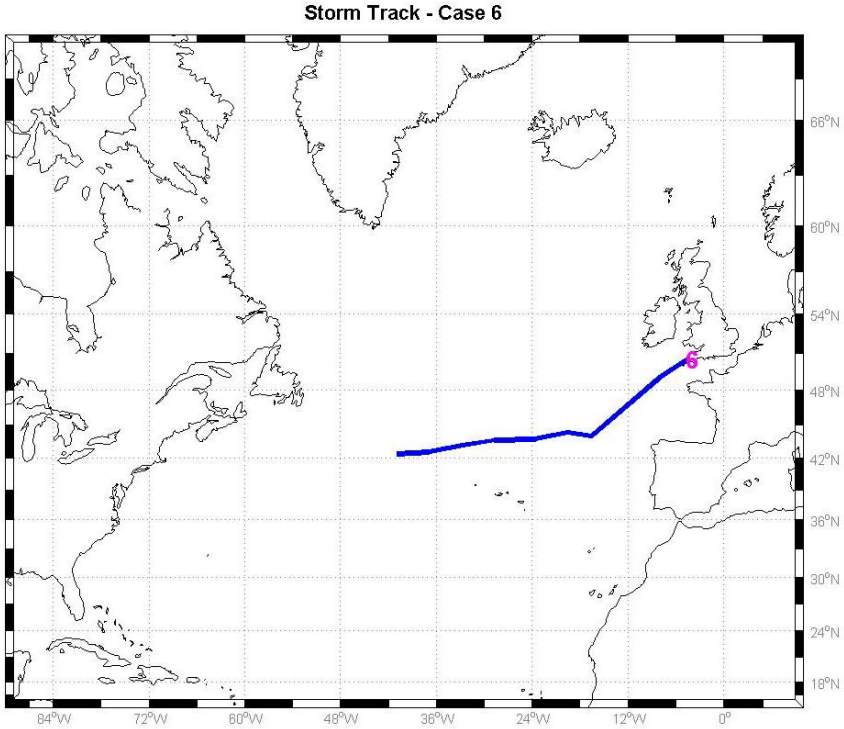

Figure 26. Case 6 – storm track from 22/12Z to 27/00Z.

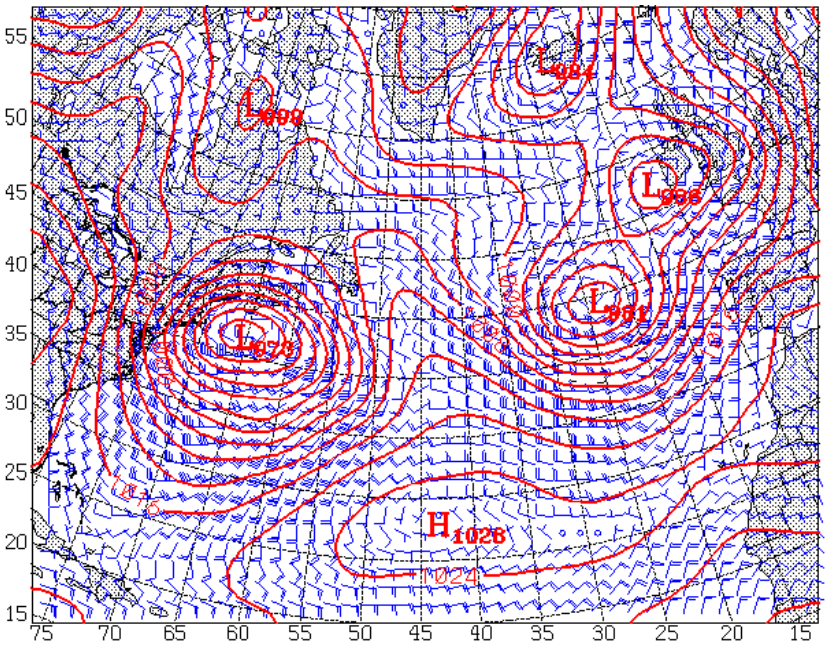

Figure 27. Case 6 – synoptic picture at 26/06Z.

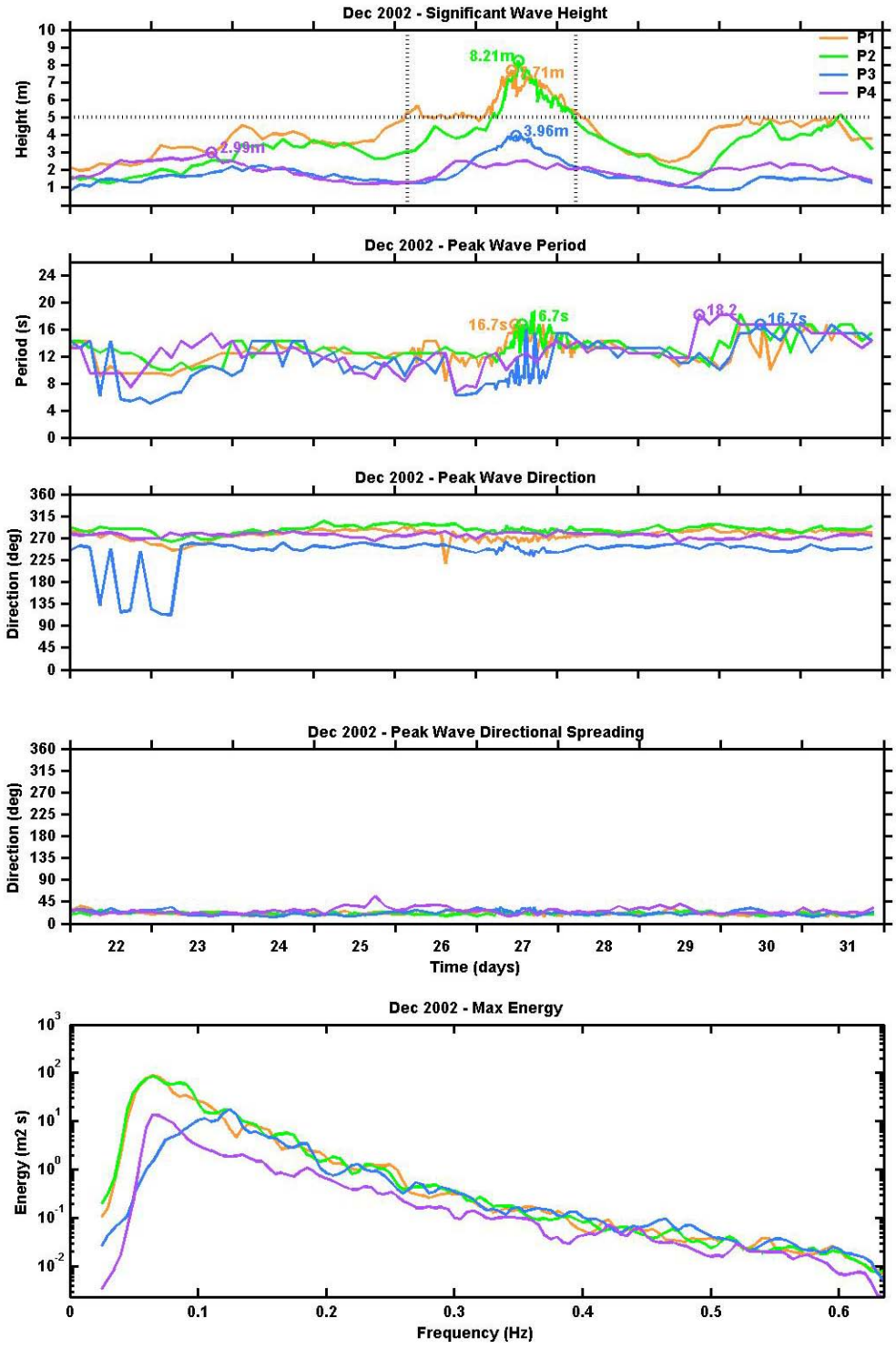

Figure 28. Case 6 – wave parameters.

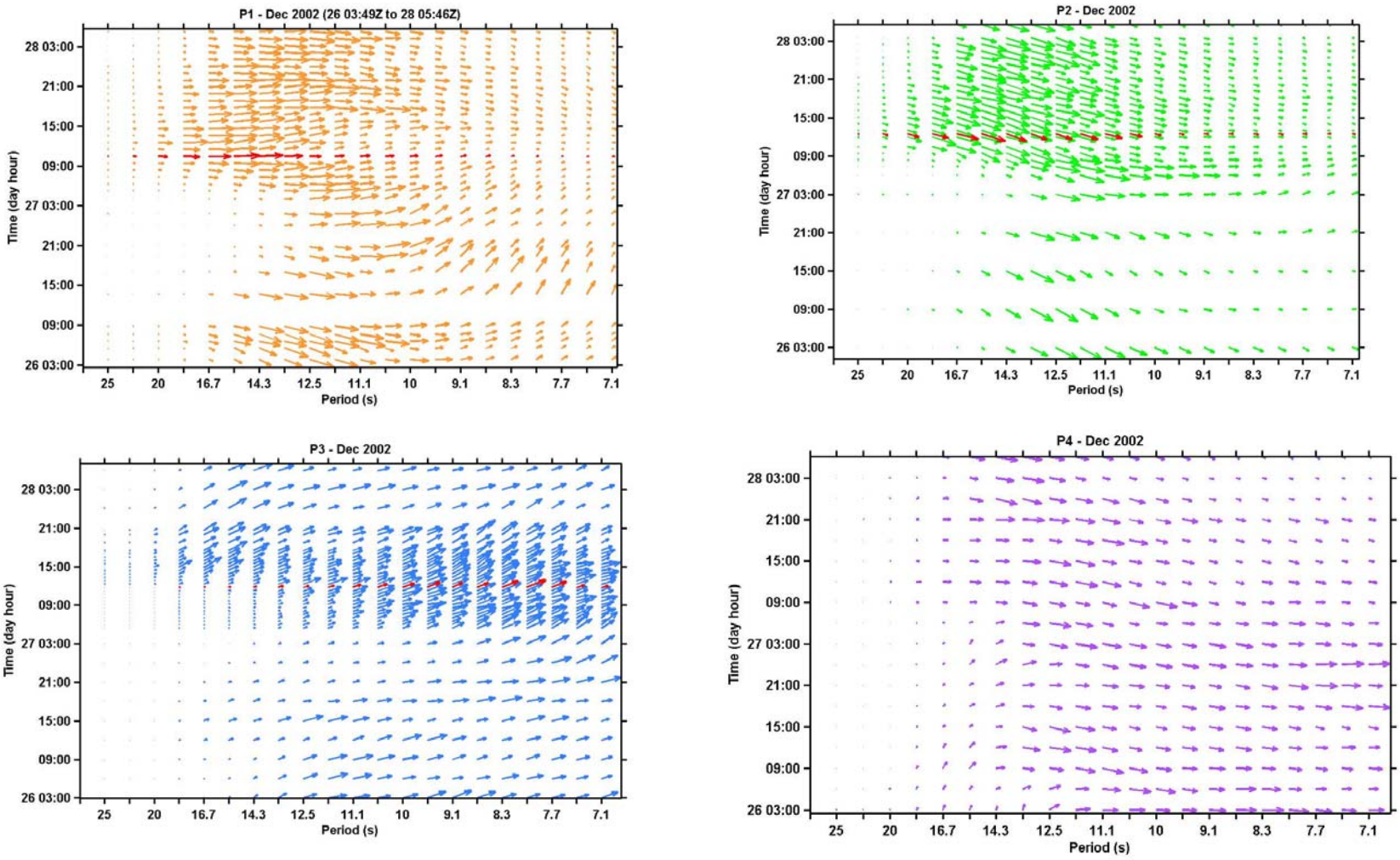

Figure 29. Evolution of energy density (arrow length logarithmically scaled) and mean direction (at each frequency) during storm case 6. Time of maximum energy indicated in red.

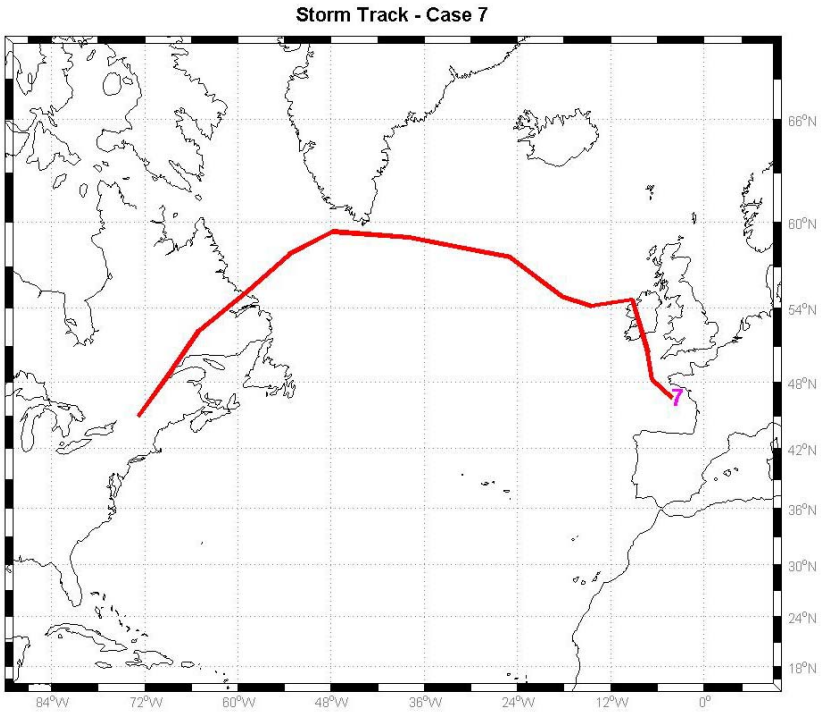

Figure 30. Case 7 – storm track form 28/00Z to 01/06Z.

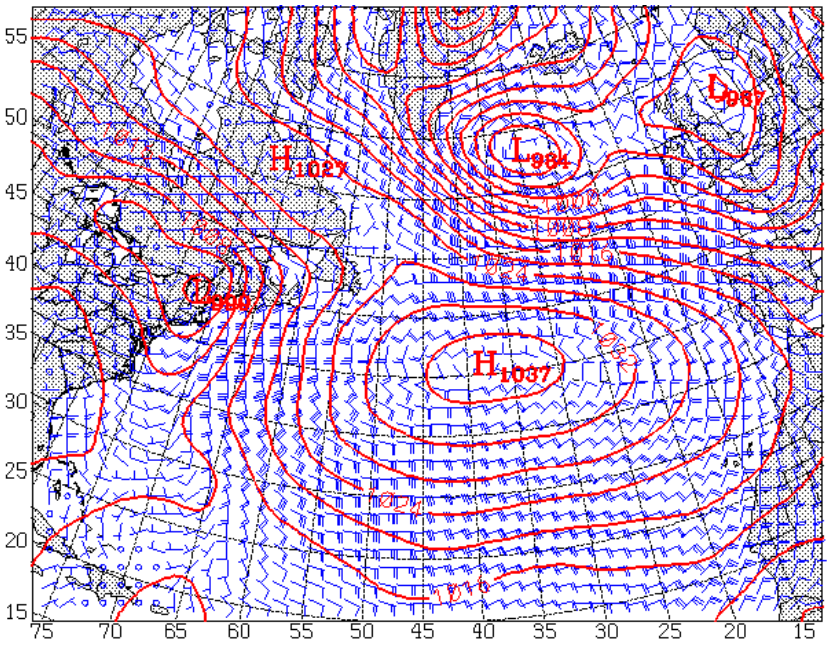

Figure 31. Case 7 – synoptic picture at 30/00Z.

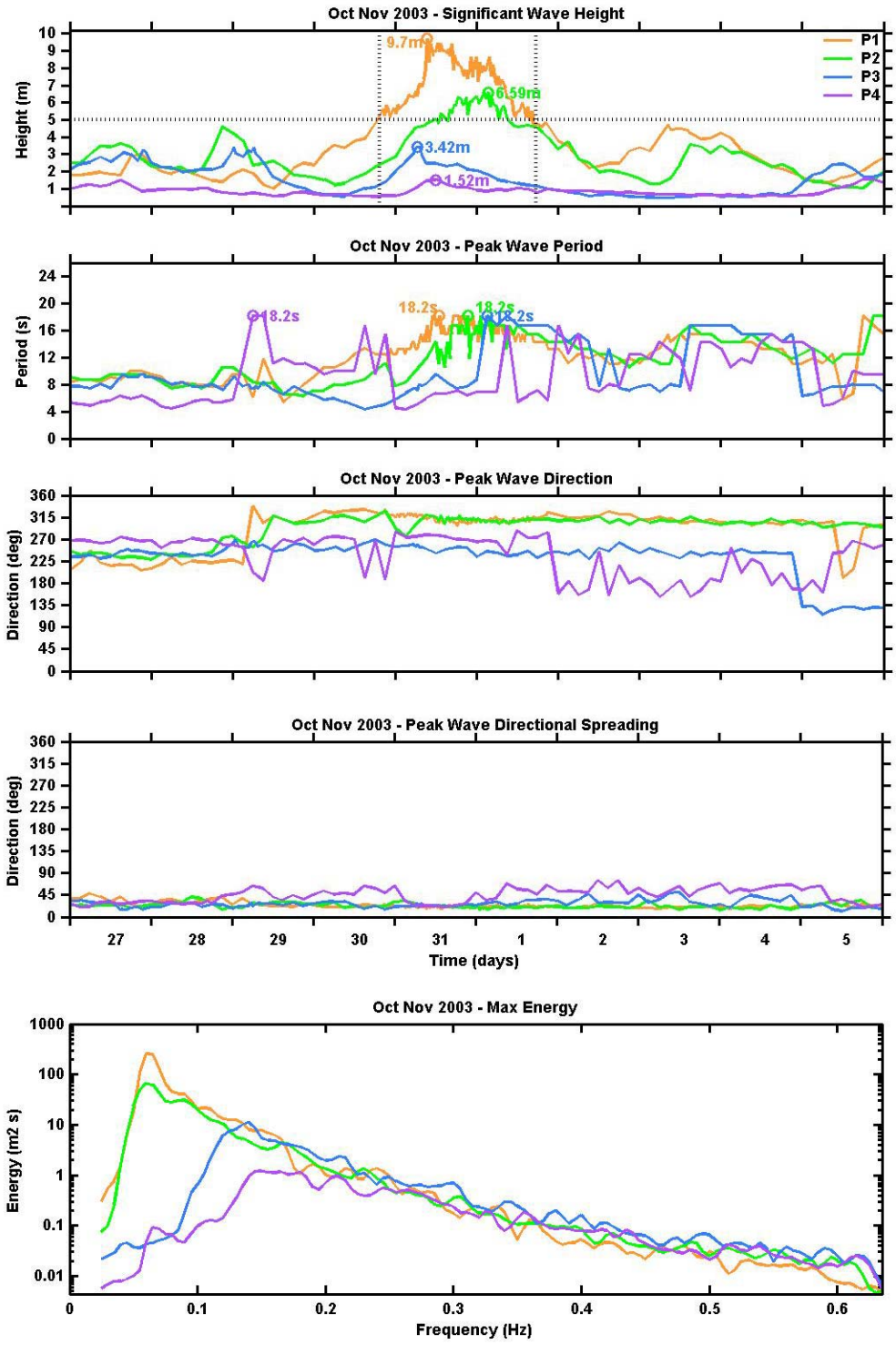

Figure 32. Case 7 – wave parameters.

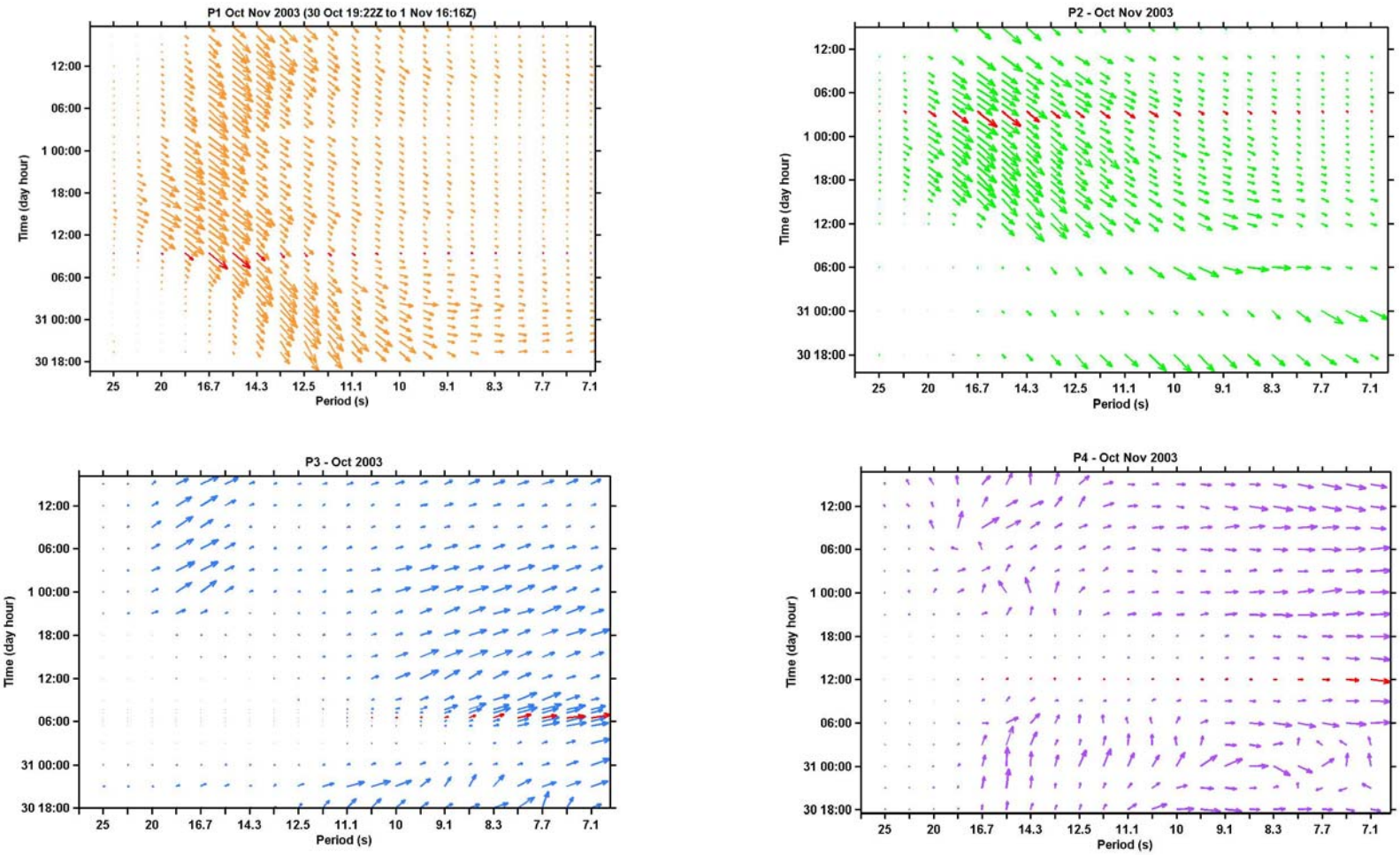

Figure 33. Evolution of energy density (arrow length logarithmically scaled) and mean direction (at each frequency) during storm case 7. Time of maximum energy indicated in red.

IV. WAVE MODEL HINDCASTS

A. HINDCASTS

To validate the application of the WAVEWATCH III model to the extreme wave events off the Portuguese coast, and examine the spatial structure of the wave fields in relation to the storm characteristics, model hindcasts were performed for two of the case studies. Cases 6 (negative NAO) and 7 (positive NAO) were selected.

The WAVEWATCH III domain used in the hindcasts covered a large part of the North Atlantic basin, from 20° N to 60° N, and from 0° to 85° W, with a 0.25 degree grid spacing. The wave spectra were discretised into 24 directions and 25 frequencies. The directions start at true north and encompass 360° clockwise in increments of 15°. The frequencies were logarithmically incremented by a factor of 1.1.from 0.0418 hertz. A 15 minutes time step was used for integrating both the propagation and the source terms. In both cases WAVEWATCH III was initiated in a cold start, with no pre-existing wave field present. In order to allow for a period of spin-up, the model runs were started four days prior to the ten day analysis period. The model was set-up without subgrid scale parameterization or ice background. In order to allow for a comparison between the model output and the buoy observations, the four grid points, closest to the buoys E1, P1, P2 and P3, were selected.

1. Hindcast 1 – Case 6

The time history of significant wave height, peak wave period and peak wave direction for the buoy observation and

hindcast 1 are compared in Figures 34, 35 and 36. The comparison of energy spectra at the time of the highest significant wave height is shown in Figure 36.

The model generally reproduces the wave height evolution observed at the buoys located on the west coast of the Iberian Peninsula (E1, P1 and P2), but slightly overestimates the maximum significant wave height at all three locations. The errors are within the roughly 15 percent tolerance margin of WAVEWATCH III predictions that is considered acceptable in typical open ocean applications (Wittmann, personal communication, 2005). At buoy E1 the prediction error was about 9.4 percent, but the storm peak time was predicted about three hours earlier than observed. At buoys P1 and P2 the model predictions were better, with an error of 2.3 percent and less than 2 percent, respectively. For both these buoys, the predicted time of maximum wave height was close to that observed. However predictions of significant wave height at buoy P3 (located on the south coast) are considerably less accurate, where the predicted peak is about 5 hours late with an error of about 12.5 percent.

The predictions for the peak period followed a similar pattern as the significant wave height. At buoys E1, P1 and P2, the peak period prediction followed the buoy observations closely, especially during the storm period. At buoy P3 the model slightly overpredicted the peak period. The predicted peak wave directions are close to the observations at buoys P1 and P2 but about 45 degrees off at buoy P3. There was no directional data available at buoy E1.

The predicted energy spectra (at the time of maximum wave height) at buoys E1, P1 and P2 are also close to the observations. The predicted spectrum at buoy P3 is less accurate than those at the western coast buoys. The energy at higher frequencies is underpredicted, suggesting that the model didn't resolve adequately the presence of locally generated wind seas.

2. Hindcast 2 – Case 7

The time histories of significant wave height, peak wave period and direction, and energy spectra (at the time of maximum wave height) are shown in Figures 38 to 41.

The predictions of the maximum significant wave height are less accurate than in hindcast 1. At buoy E1 WAVEWATCH III overpredicted the maximum significant wave height by about 22 percent, but predicted the arrival time correctly. At buoy P1 the error is significantly less (4.5 percent), but with an 8 hour lag of the peak wave arrival time. At buoy P2 the model overpredicted the maximum significant wave height by about 17 percent. The storm peak at this buoy was reasonably well predicted. At buoy P3, as in the previous hindcast, the model didn't handle the significant wave height prediction as well as at the other three buoys, with an error of about 35 percent. This large error in this case may be related to the fact that the prevailing incoming swell direction was from the northwest, whereas in the previous case it was from the west. The swell propagation around the southwest tip of Portugal (Cape *Sao Vicente*) into the shadow zone where buoy P3 is located (Figure 3) is not well represented in the

current implementation of WAVEWATCH III on a relatively coarse grid that does not account for nearshore refraction effects.

As in hindcast 1, the model predictions for the peak period are accurate at buoys E1, P1 and P2. The accuracy of predicted peak wave direction is similar to hindcast 1, i.e., good at buoys P1 and P2 and poor at buoy P3. No direction data was available at buoy E1.

The significant wave height overprediction at buoy E1 is associated with an overprediction of the peak spectral level (Figure 41). This overprediction was less pronounced at buoys P1 and P2. The energy spectrum prediction at the buoy P3 is poor. The model underprediction of energy density at higher frequencies is higher than in hindcast 1, again suggesting that the model does not capture local wind seas. A more serious discrepancy is noted at the swell peak which is not predicted by the model. As discussed earlier, a higher resolution model with refraction is needed to handle the propagation of swell around the south-west tip of Portugal.

B. WAVE FIELDS

The good overall performance of the model WAVEWATCH III in the two hindcasts gives confidence in the predicted wave fields. In Figures 42 and 43 the wave fields for cases 6 and 7 are shown, respectively, together with the cyclone track. In case 6, the significant wave height was more uniform along the west coast of the Iberian Peninsula and more intense on the south coast of Portugal. On the other hand, in case 7, the high swell was more concentrated

on the northern coast of Portugal and Galicia, and the south coast of Portugal was more sheltered.

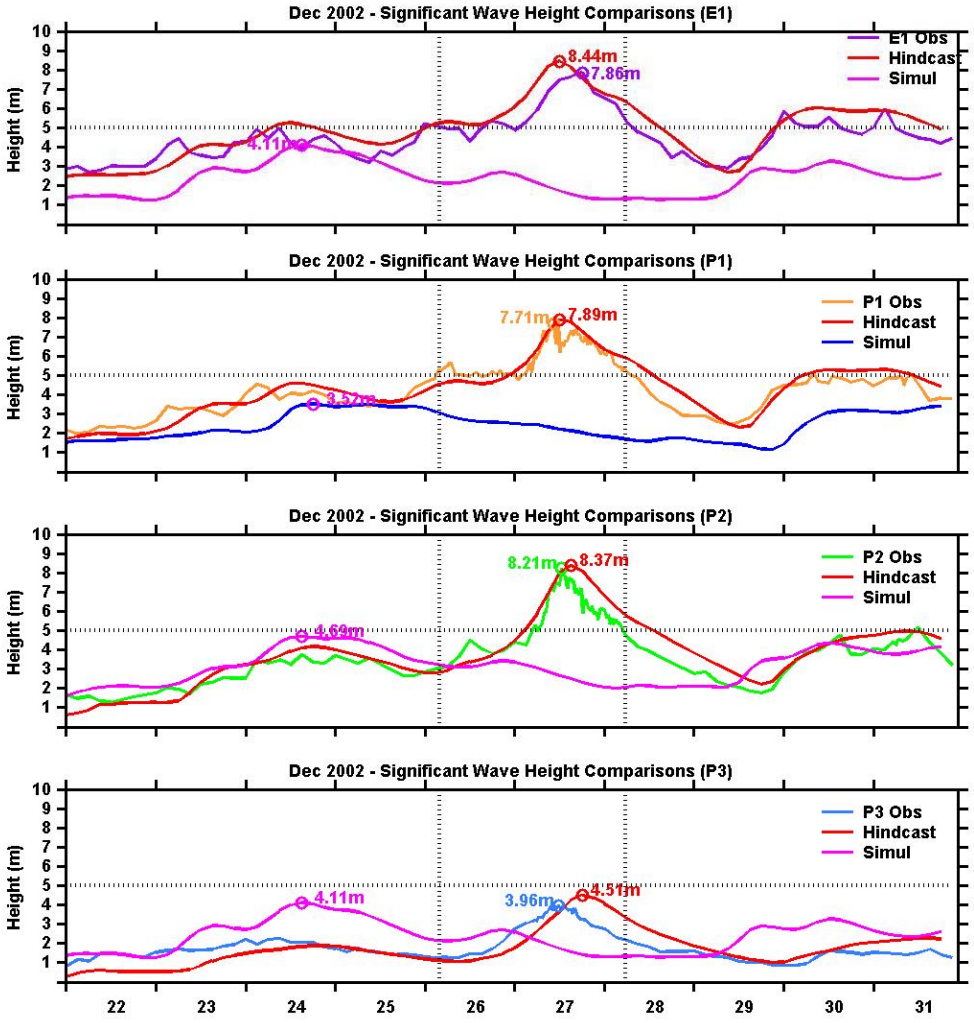

Figure 34. Case 6 - significant wave height comparisons.

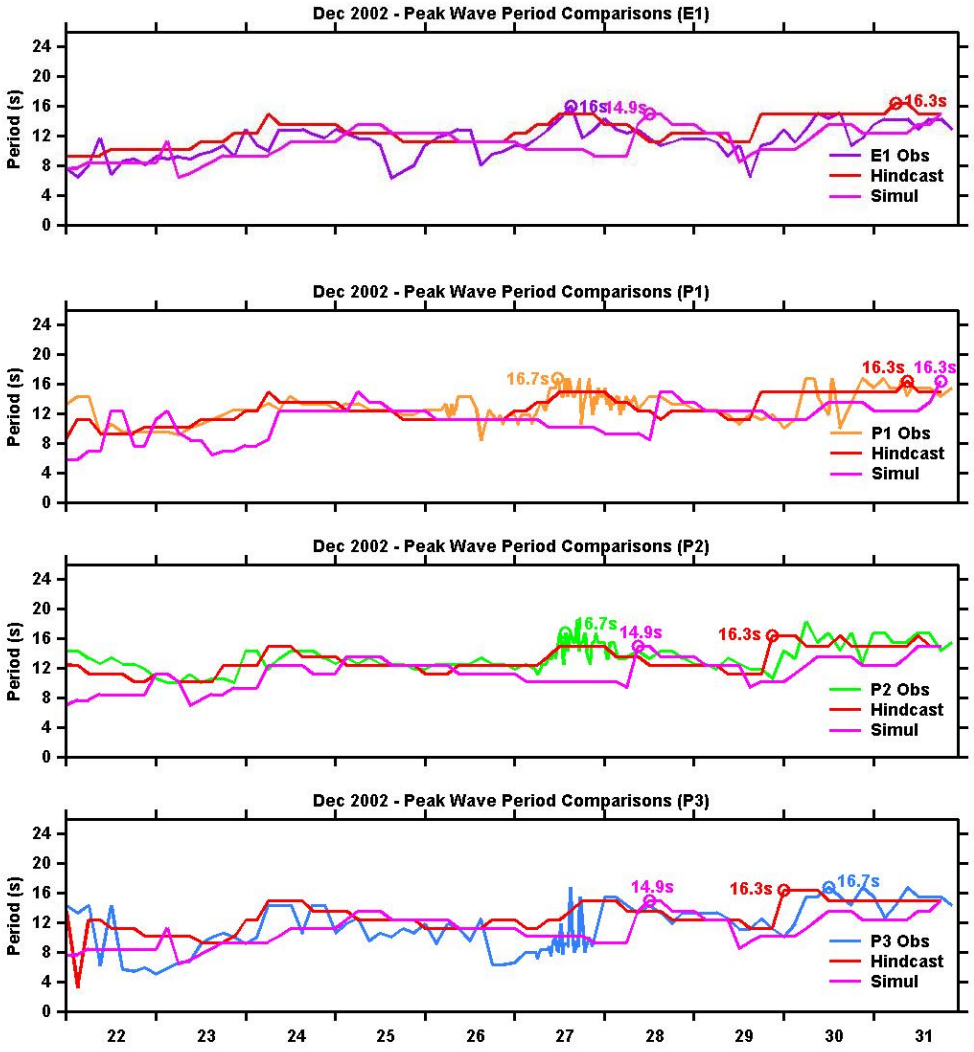

Figure 35. Case 6 - peak period comparisons.

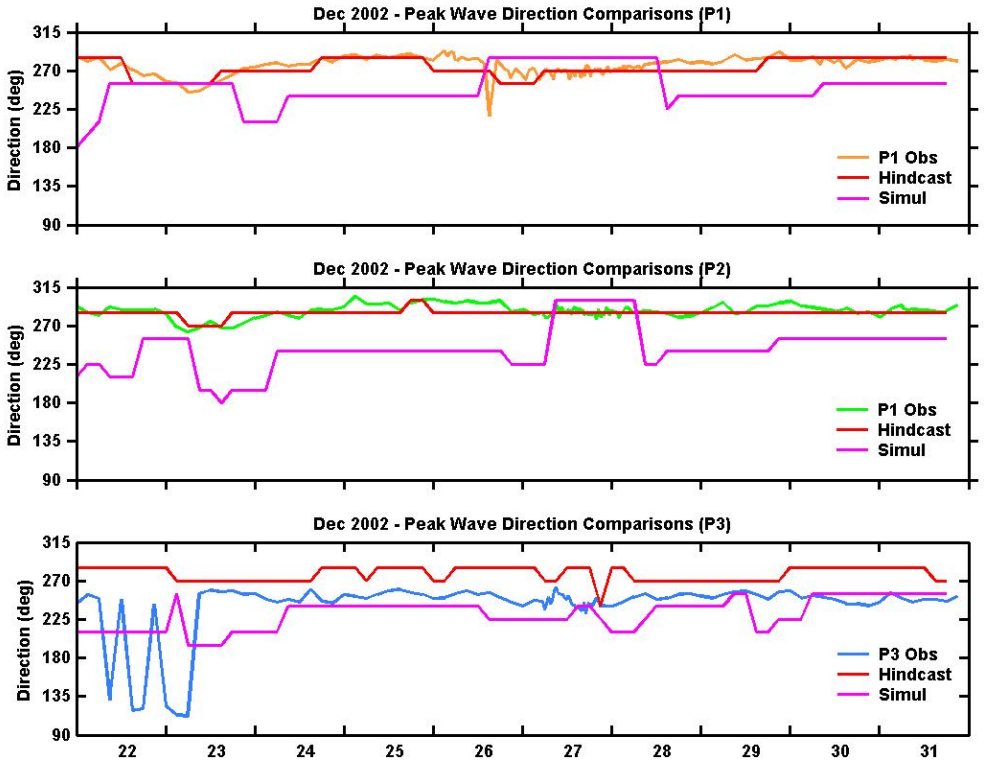

Figure 36. Case 6 - peak wave direction comparisons.

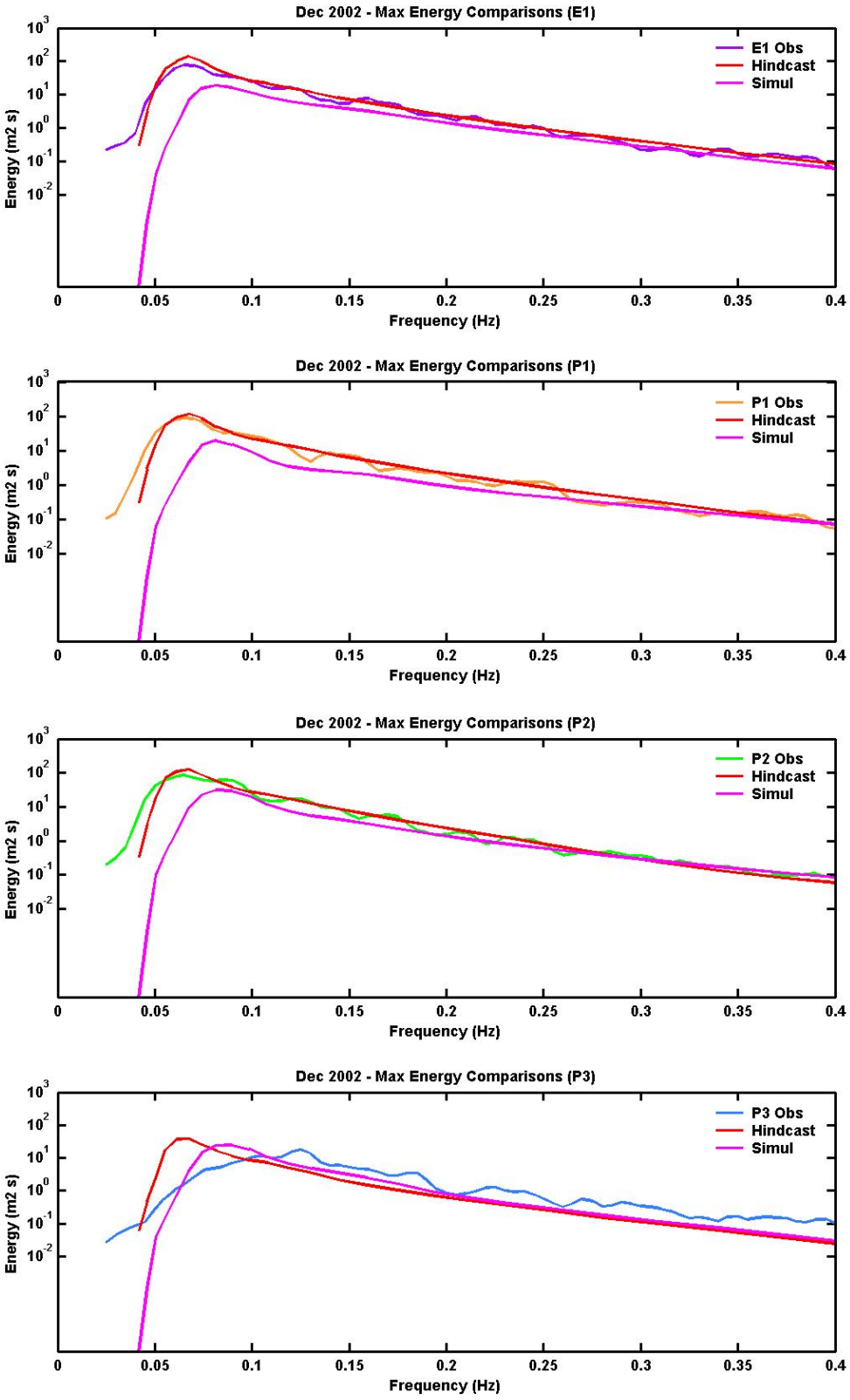

Figure 37. Case 6 - energy spectra comparisons.

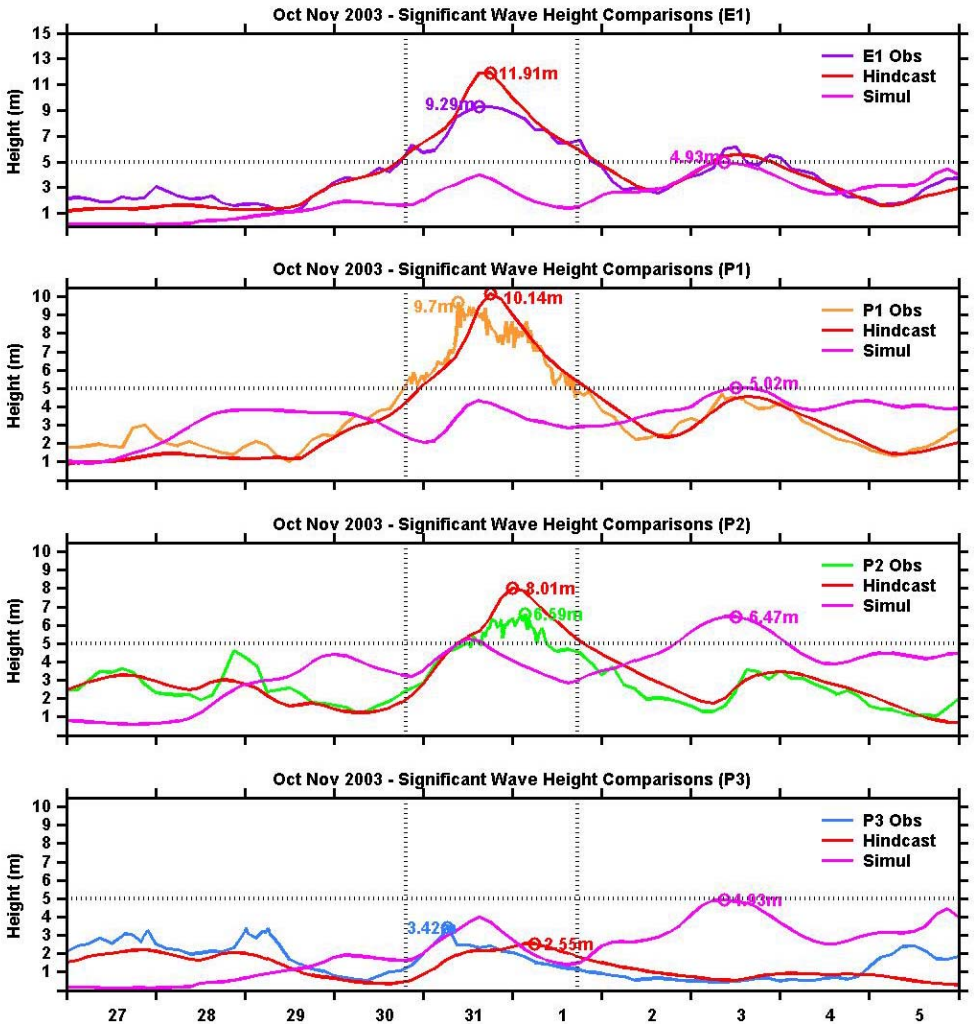

Figure 38. Case 7 - significant wave height comparisons.

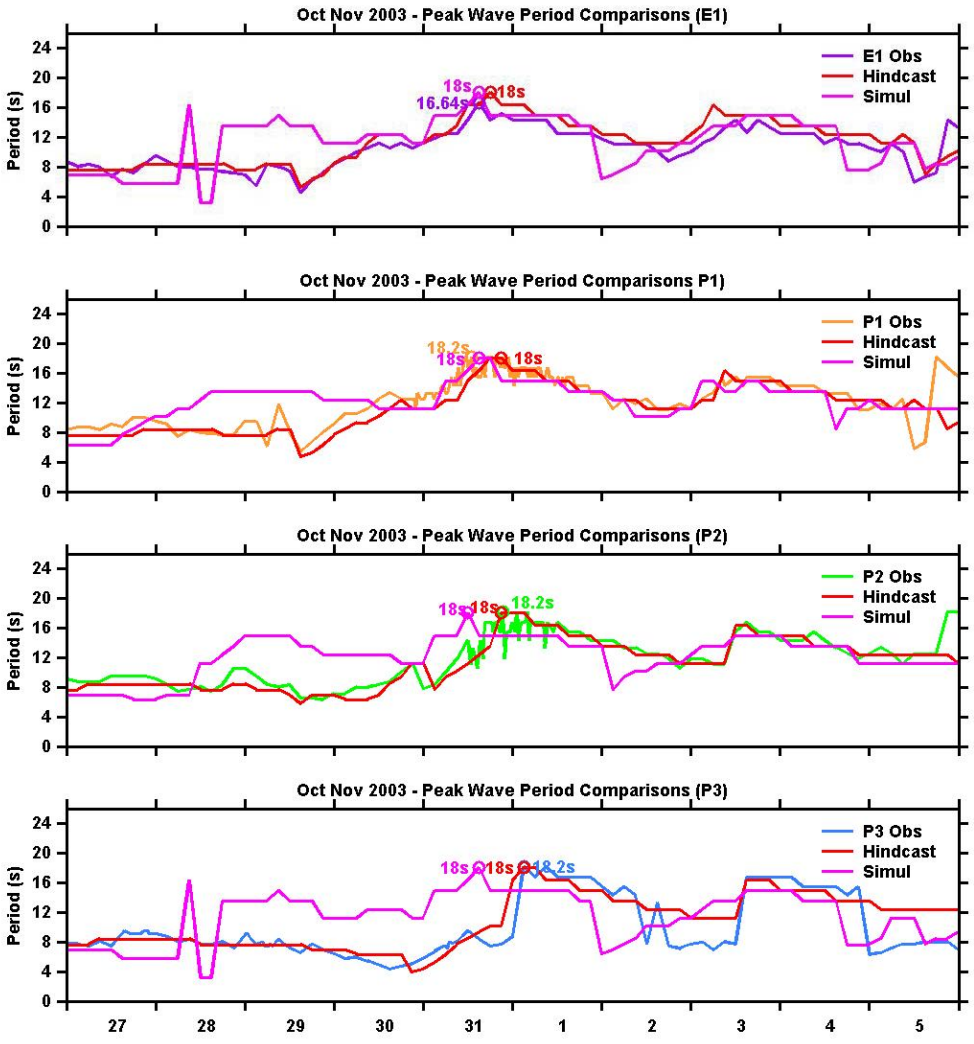

Figure 39. Case 7 - peak period comparisons.

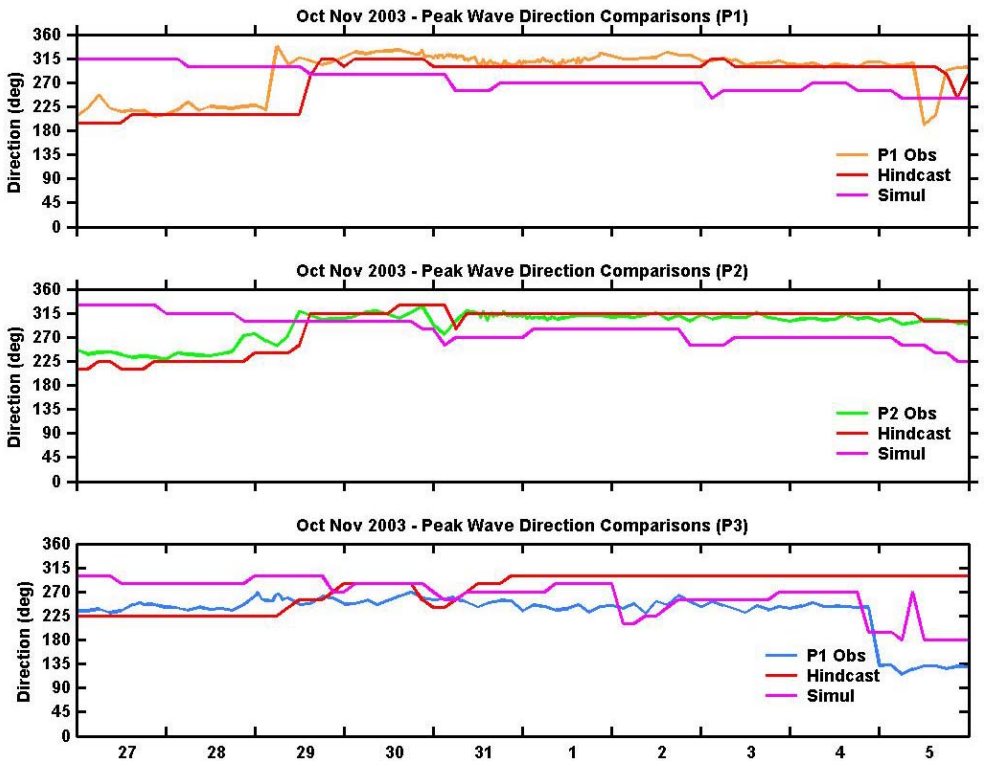

Figure 40. Case 7 - peak wave direction comparisons.

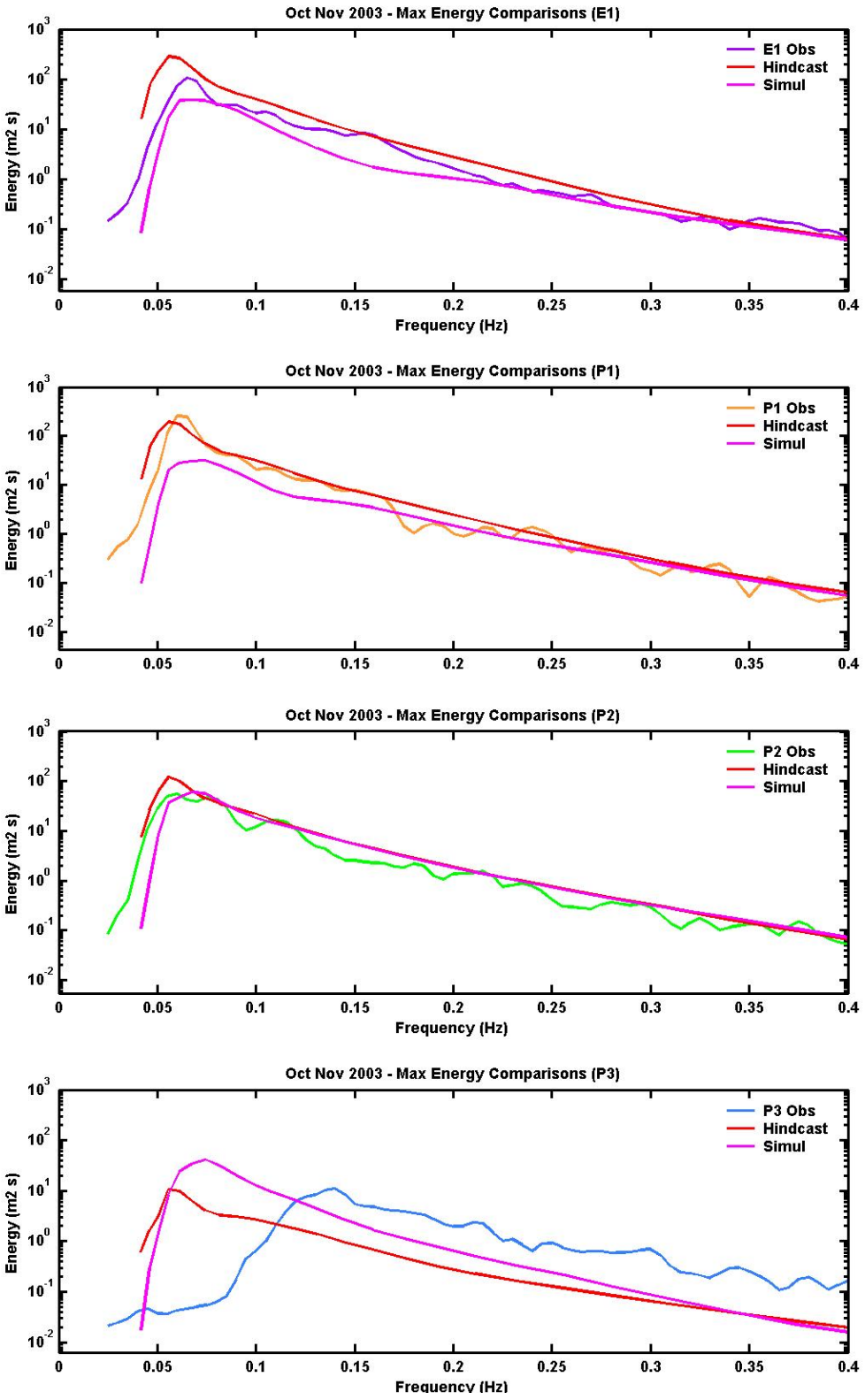

Figure 41. Case 7 - energy spectra comparisons.

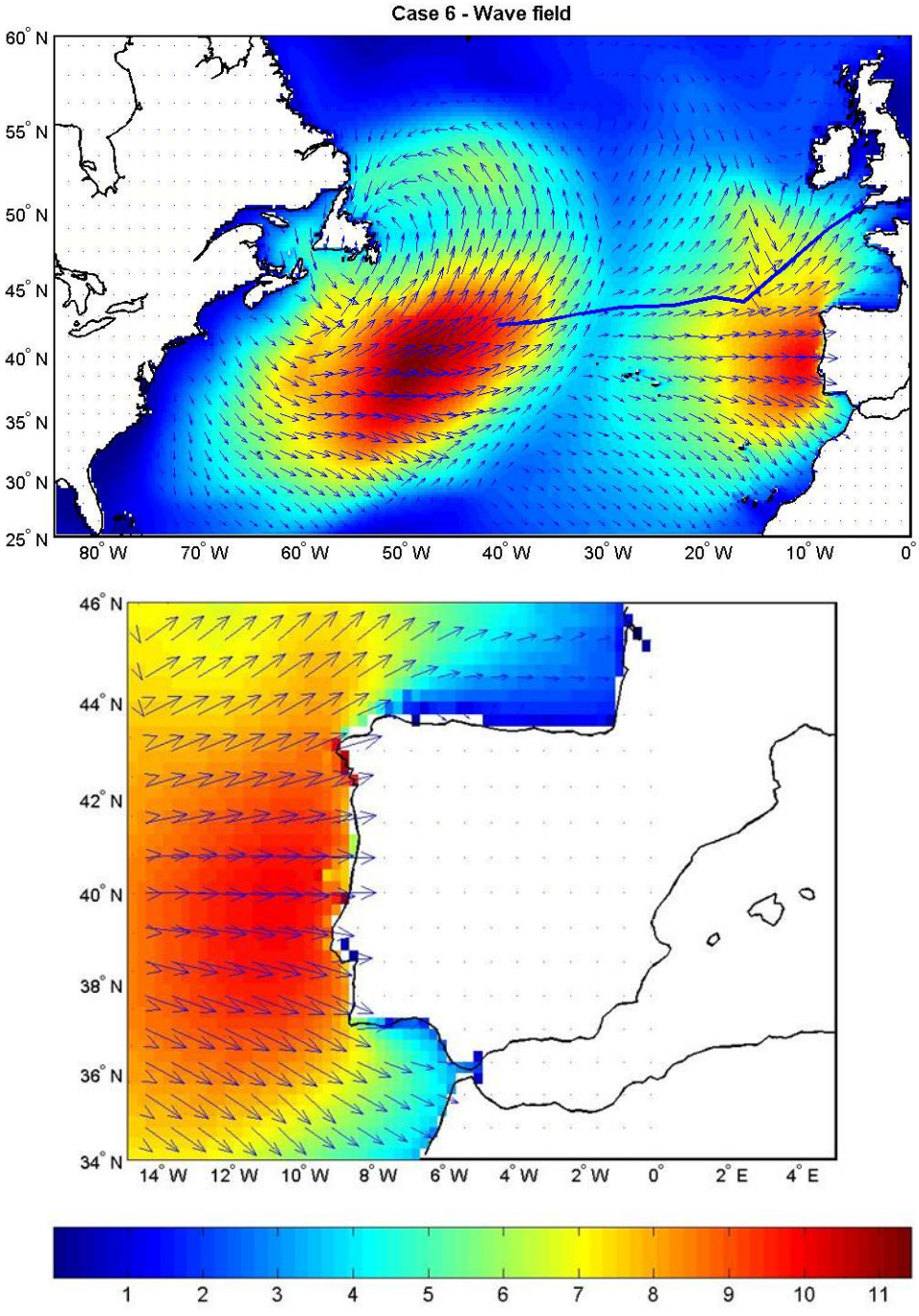

Figure 42. Case 6 - significant wave height and peak wave direction fields.

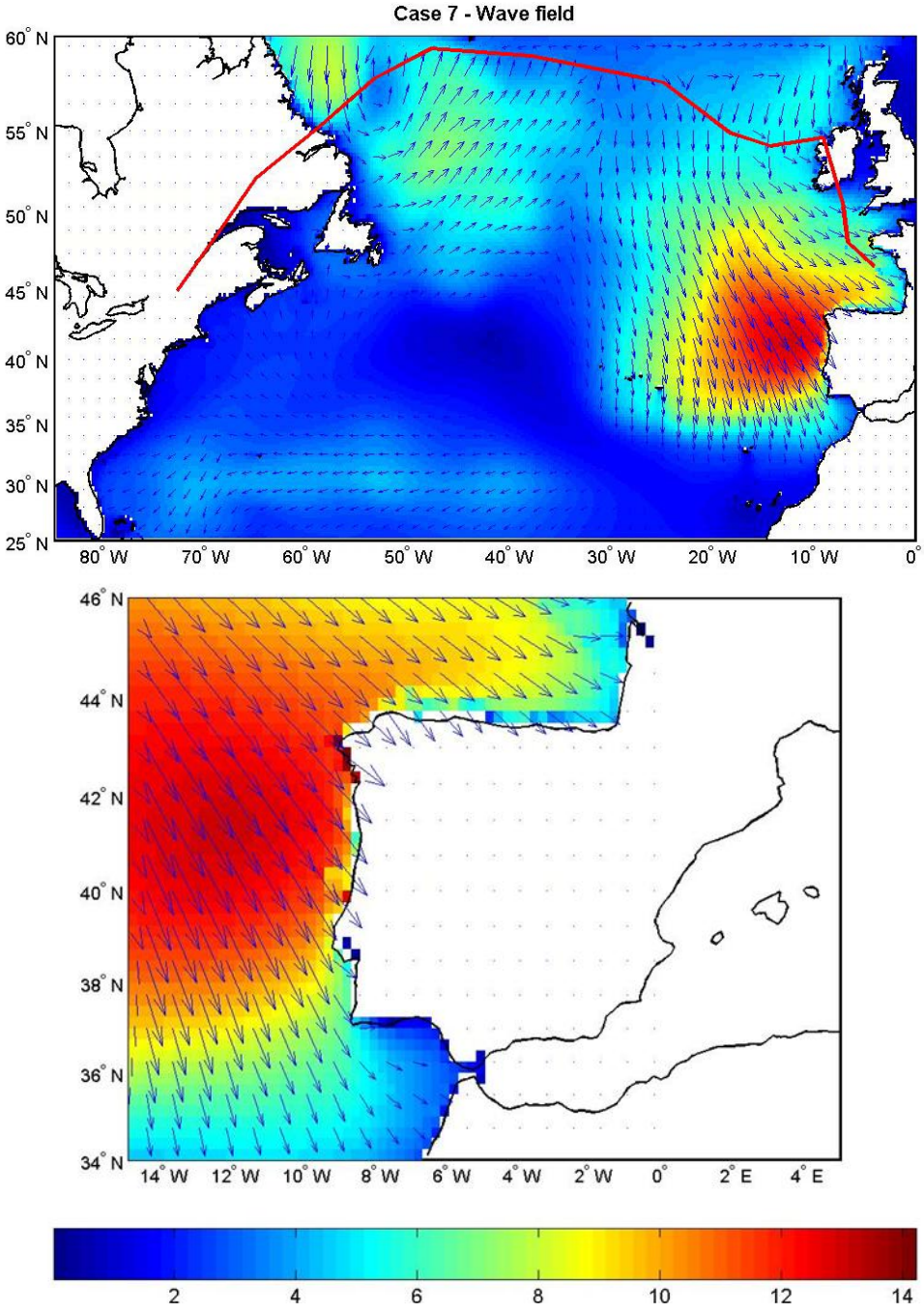

Figure 43. Case 7 - significant wave height and peak wave direction field.

THIS PAGE INTENTIONALLY LEFT BLANK

V. DISCUSSION

In the following, reference will be made to the seven cases described in the preceding section, trying to establish a connection between the NAO phase and the storm tracks and the characteristics of the wave regime off the coast of Portugal. From the seven cases selected for this study, three were classified as positive NAO storms and four as negative NAO storms (Table 3), based on the ten day NAO index previously defined (Figure 5).

All storms, with the exception of case 5, lasted around two days. The storm in case 3 was slightly shorter (38 hours and 50 minutes). But in the three days prior to the beginning of case 3, the measured significant wave height at buoy P1 was consistently higher than 4 meters, and occasionally higher than 5 meters. Thus, since the duration of storms is similar in six of the seven cases, there appears to be no relationship between the duration of the storms and the NAO phase. All storms were of longer duration at the northern-most buoy. In fact, swell higher than 5 meters was always recorded first on buoy P1, followed by buoy P2, and wave heights higher than 5 meters were never recorded at buoys P3 and P4.

In Table 5, the seven case studies were re-ordered by the ten day NAO index, from the highest (more positive) to the lowest (more negative). The maximum significant wave height at buoy P1 decreased with the NAO strength, with the exception of case 3 (Figure 44). At buoy P2 the trend was less clear and inverse: the maximum significant wave height

at buoy P2 increased as the NAO strength decreases, with the exceptions of cases 1 and 2.

There is a clear relation between the NAO strength and the relative storm intensity at buoys P1 and P2. For the positive cases (1, 3 and 7), the waves were more intense on the northern part of the west coast of Portugal, where buoy P1 was moored. In each one of these positive cases, the significant wave height measured at buoy P1 was consistently higher than at buoy P2. The maximum significant wave height was 2.34 meters higher at buoy P1 in case 1, 0.85 meters higher in case 3 and 3.11 meters higher in case 5. For the remaining four negative cases (i.e., cases 2, 4, 5 and 6), the maximum significant wave height was higher at buoy P1 in two of them (0.67 meters in case 5 and 0.48 meters in case 6) and higher at buoy P2 for the remaining two most negative cases (0.5 meters and 1.78 meters in cases 6 and 2, respectively).

Case	10 day NAO index	Significant wave height – P1 (m)	Significant wave height – P2 (m)	Difference P1 – P2
7	0.9718	9.70	6.59	3.11
1	0.6634	8.76	6.42	2.34
3	0.5155	8.80	7.95	0.85
4	-0.4441	7.81	7.14	0.67
5	-0.7115	7.72	7.24	0.48
6	-1.2610	7.71	8.21	-0.50
2	-1.5953	6.27	7.65	-1.38

Table 5. Relation between the ten day NAO index and the maximum significant wave height at buoys P1 and P2.

The relation between the peak wave direction at the peak of the storm at buoys P1 and P2, and the NAO strength, was less clear. Nevertheless, the general pattern appears to be that the stronger the NAO, the closer the peak wave direction at buoys P1 and P2 was to northwest (i.e., 315 degrees from true north). As expected for northeast tracking storms (Table 6 and Figure 34). On the other hand, with a weaker NAO, which corresponds to a more zonal storm tracking, the wave directions were closer to 270 degrees (Table 6 and Figure 41). An exception to this trend was case 3, with a moderate positive NAO index but a westerly peak wave direction (286 at buoy P1 and 295 at buoy P2). One factor that may have contributed to this situation was the unusual north-south width of this storm as it tracked across the North Atlantic basin, thereby contributing to the development of a more westerly oriented prevailing fetch Another exception to this pattern occurred in case 2 with a large negative NAO index but a northwesterly wave direction at buoy P1. This can be explained by the fact that the largest waves arrived at buoy P1 about two days earlier than at buoy P2, and included older northwest swell (Figure 12).

Case	10 day NAO index	Peak wave direction - P1	Peak wave direction - P2
7	0.9718	311	308
1	0.6634	318	312
3	0.5155	286	295
4	-0.4441	295	303
5	-0.7115	281	298
6	-1.2610	268	288
2	-1.5953	298	286

Table 6. Relation between the ten day NAO index and the peak wave direction at buoys P1 and P2.

As for the sheltered P3 and P4 buoys, the relation between the NAO phase, the significant wave height and the peak wave direction was not as clear. The highest recorded significant wave heights at buoy P3 (close to 4 meters) occurred in three of the four negative cases (cases 2, 4 and 6), consistent with the fact that the south coast of Portugal is exposed to west swells from more south tracking storms, while sheltered from northwest swell (Table 7 and Figure 45). The exception was case 5 (a negative case), where the maximum significant wave height was lower than for any of the three positive cases. This cyclone followed an unusual path, tracking zonally, from the east coast of the US towards the Azores, and then northwesterly, towards the British Islands (Figure 22). The highest significant wave heights at buoy P4 occurred in the two most negative cases (2.99 meters in case 6 and 2.81 meters in case 2) and the lowest in the two most positive cases (1.52 meters in case 7 and 1.48 in case 3 – Table 7 and Figure 45), again

in agreement with coastal sheltering from north tracking storms (with a positive NAO index).

Case	10 day NAO index	Significant wave height – P3 (m)	Significant wave height – P4 (m)	Peak wave direction – P3 (deg)	Peak wave direction – P4 (deg)
7	0.9718	3.20	1.52	260	280
1	0.6634	2.62	1.48	255	-
3	0.5155	3.89	2.51	219	283
4	-0.4441	4.01	2.27	261	265
5	-0.7115	2.64	-	231	-
6	-1.2610	3.96	2.99	248	275
2	-1.5953	4.10	2.81	257	285

Table 7. Relation between the ten day NAO index and the maximum significant wave height and peak wave direction at buoys P3 and P4.

To examine the relation between the pathway of the storms and the NAO strength, the storm tracks corresponding to the seven case studies were plotted together on a map (Figure 46). The red and orange tracks correspond to the positive case studies (cases 1, 3 and 7), and the blue tracks correspond to the negative case studies (cases 4, 5, 6 and 2). With the exception of case 1, all positive storms tracked further north than the negative NAO storms. Case 5 tracked more northeast than any other negative case, but the low was originated farther south than on any other case, with the exception of case 2 (an extra-tropical transition case). The low on case 2 tracked northeast until the middle of the North Atlantic, and then southeast and east. Only case 2 (the most negative) had a low occluding

in the Iberian Peninsula. The lows in the remaining negative cases occluded in the Celtic Sea or in the Southern part of England.

The influence of the cyclone tracking, and therefore of the NAO strength, on the wave field characteristics was examined with hindcasts in the previous chapter. In case 6 (negative), the highest swell off the Iberian Peninsula was generated during the zonal path of the mid-latitude cyclone, before it shifted towards the British Islands (Figure 26). The result was a more evenly distributed wave field across the west coast of Portugal and Galicia. Case 7 (positive) had a low tracking northwest from New England and then, after it reached the south of Iceland, to the southeast due to a blocking pattern in the central North Atlantic. The highest swell that reached the Iberian Peninsula in this case study was generated when the low was tracking northeast. The result in terms of wave field was higher waves in the northern part of the west coast of Portugal, where buoy P1 was moored, and smaller waves on the southern west coast, where buoy P2 was moored. The wave field on the southern coast of Portugal, where buoy P3 was moored, confirmed the importance of the sheltering of the south coast of Portugal from northeast tracking storms.

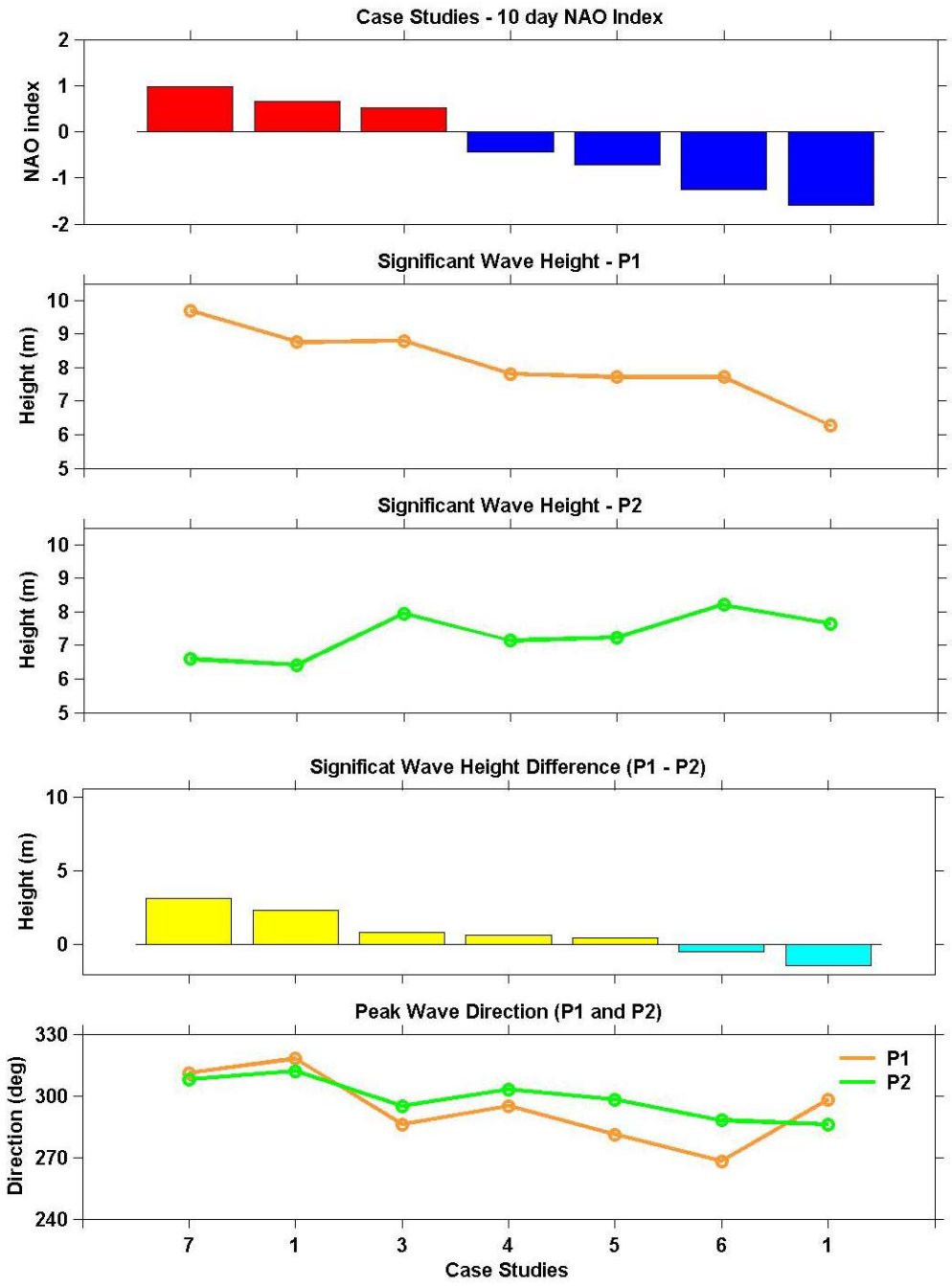

Figure 44. Ten day NAO index, significant wave height and peak wave direction at buoys P1 and P2.

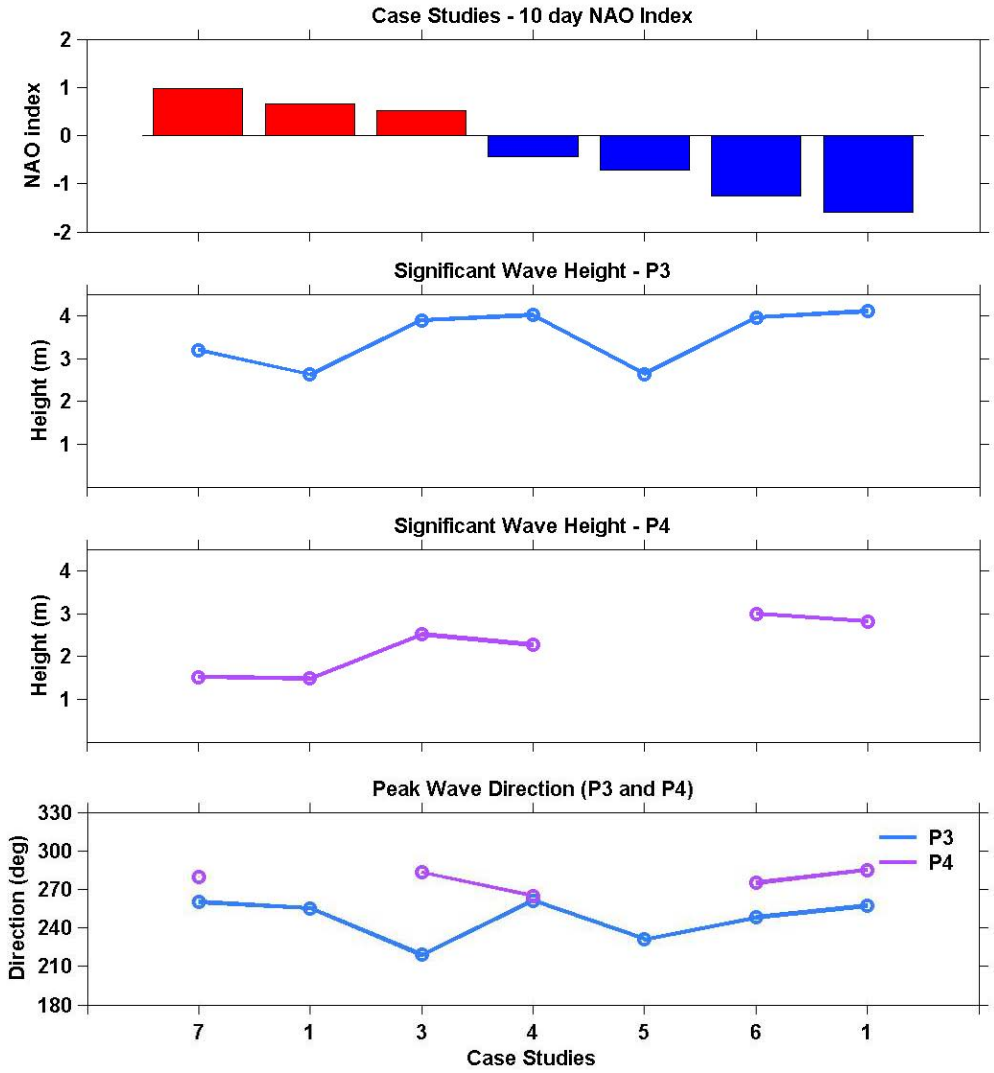

Figure 45. Ten day NAO index, significant wave height and peak wave direction at buoys P3 and P4.

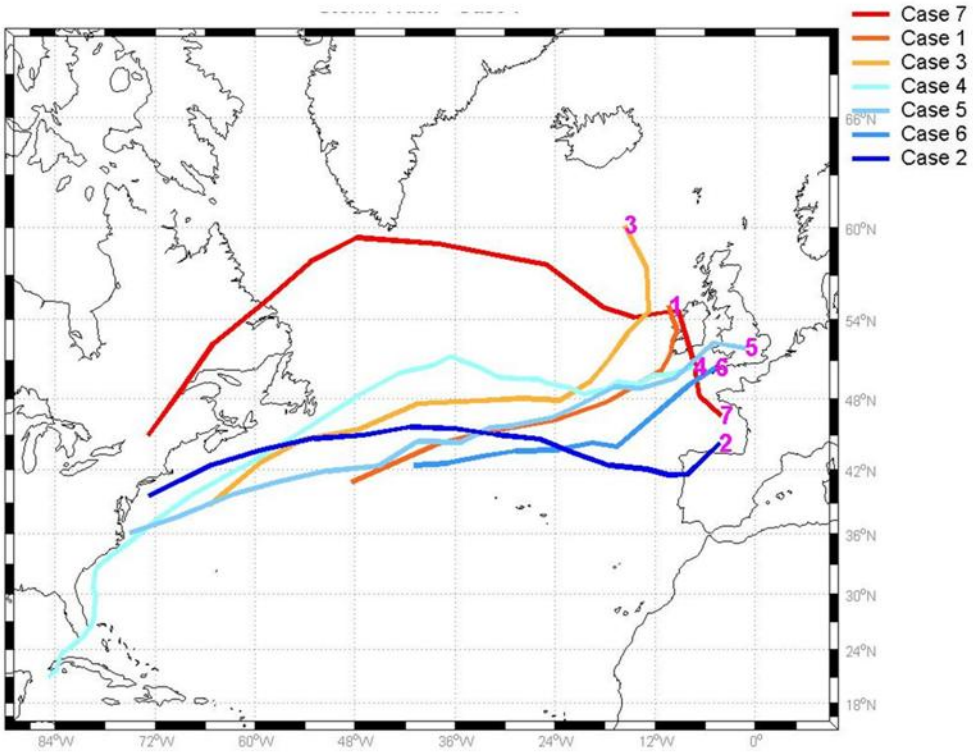

Figure 46. Storm tracks.

THIS PAGE INTENTIONALLY LEFT BLANK

VI. CONCLUSIONS AND RECOMENDATIONS

A. CONCLUSIONS

The aim of this study was to gain a greater understanding of the wave regime in Portugal as a function of the North Atlantic Oscillation phase. The results confirmed the importance of the NAO to the characteristics of the swell regime off the coast of Portugal, a consequence of the NAO's close relationship to the storm tracks across the North Atlantic basin. Seven case studies were selected, based on extreme wave heights measured at two buoys moored on the western coast of Portugal's mainland, and in accordance with a previously chosen selection criteria. These seven cases were then related to the NAO phase, based on a ten day index computed for each case.

No relation between the storm duration and the NAO phase was found. On the other hand a clear relationship between the wave height variations along the west coast of Portugal (where buoys P1 and P2 were moored) and the NAO phase was found. For strong positive NAO storms, larger swell were observed at the northern buoy (P1), whereas in weakened NAO phase storms, the wave heights were more uniform and sometimes higher at the southern buoy (P2). A relationship between the incoming swell direction at buoys P1 and P2 and the NAO phase was also found. As the NAO weakened the swell directions consistently shifted from northwest to a more westerly direction, in agreement with the shifting in the storm tracks. Thus, storms tracking northeast, characteristic of positive NAO events, generate

northwest swell throughout the west coast of Portugal. On the other hand swell from the west is to be expected in negative NAO events, as a result of storms tracking more zonally.

The relationship between the characteristics of the wave regime at buoys P3 and P4 (moored at the south coast of Portugal and south of Madeira Island, respectively) and the NAO phase was less clear, due to the fact that these buoys were sheltered from the prevailing swell direction. The wave heights at these buoys were higher during negative, that is zonally tracking, NAO storms, when the prevailing swell arrived from the west, and were less affected by the southern tip of Portugal.

B. RECOMMENDATIONS FOR FUTURE RESEARCH

Although this study covered a fair number of case studies, the expansion of the analysis period from ten years to all buoy data available at the *Instituto Hidrografico* (more than twenty-five years) would allow a better characterization of the storm-wave climatology. The study should also be extended to storms that occurred in strong or weak NAO periods and that had reduced impact in the wave field off the coast of Portugal. This would allow a better understanding of the storm tracks that favor the development of large swells in Portugal.

There have been some studies that related the NAO with the occurrence of secondary lows in the North Atlantic basin and the precipitation level in Portugal. These secondary low pressure systems occur mainly in positive NAO events but are generated further south in a manner that is more common for negative NAO storms. The investigation of

the effect that these secondary lows have in terms of wave generation will allow for a more complete characterization of the wave climatology in Portugal.

The sheltering effect of the southwestern tip of Portugal precluded accurate wave predictions on the south coast of Portugal. Some refinements in the application of WAVEWATCH III in this area should be considered. The use of a finer grid and a shorter time step, or a nested grid, is needed to resolve the coastline and nearshore refraction effects. The use of a more accurate wind field in the area, based on a mesoscale model, that could potentially better describe local wind effects, should also be considered.

THIS PAGE INTENTIONALLY LEFT BLANK

INITIAL DISTRIBUTION LIST

1. Defense Technical Information Center
   Ft. Belvoir, Virginia

2. Dudley Knox Library
   Naval Postgraduate School
   Monterey, California

3. Professor Philip A. Durkee, Department of Meteorology
   Naval Postgraduate School
   Monterey, California

4. Professor Mary L. Batteen, Department of Oceanography
   Naval Postgraduate School
   Monterey, California

5. Professor Wendell Nuss, Department of Meteorology
   Naval Postgraduate School
   Monterey, California

6. Professor Thomas Herbers, Department of Oceanography
   Naval Postgraduate School
   Monterey, California

7. Dr João Teixeira
   Naval Research Laboratory
   Marine Meteorology Division
   7, Grace Hopper, Stop 2
   Monterey, California

8. Mr Paul Wittmann
   Fleet Numerical Oceanography and Meteorology Center
   Marine Meteorology Division
   7, Grace Hopper, Stop 2
   Monterey, California

9. Mr Paul Jessen, Department of Oceanography
   Naval Postgraduate School
   Monterey, California

10. Mr Bob Creasey, Department of Meteorology
    Naval Postgraduate School
    Monterey, California

11. Director-Geral do Instituto Hidrográfico
Instituto Hidrográfico
Rua das Trinas, 49
Lisboa - PORTUGAL

12. CDR Carlos Ventura Soares
Instituto Hidrográfico
Rua das Trinas, 49
Lisboa - PORTUGAL

13. Dr Nuno Moreira
Instituto de Meteorologia
Rua C ao Aeroporto
Lisboa – PORTUGAL

14. LCDR Juan Conforto
Sección de Oceanografía
Instituto Hidrográfico de la Marina
Plaza de San Severiano, 3
Cádiz – SPAIN